Chapter 3: Fundamentals of Turbulence and Boundary-Layer Theory

Dr. Bing-Chen Wang
Dept. of Mechanical Engineering
Univ. of Manitoba, Winnipeg, MB, R3T 5V6

1. Fundamentals of Turbulence

Fluid flows often exhibit **laminar** or **turbulent** patterns. Some key characteristics of these two types of flows include:

• Laminar flows exhibit regular and organized patterns and the flow pathlines are in order. In contrast, turbulent flows exhibit chaotic patterns, and flow pathlines are in disorder.

• In turbulent flows, there are eddies of different sizes interacting with each other.

• All flows (laminar or turbulent) must obey conservations laws of mass, momentum and energy.

1.1. Methodology for Studying Turbulence: from Leonardo da Vinci's Painting to Osborne Reynolds' Ground-Breaking Experiment

Turbulence phenomena are the most challenging subjects in natural science which cannot be fully-explained using any current established physical theories. Because a turbulent flow field features chaotic behaviors, the instantaneous velocity and pressure field fluctuates significantly. Therefore, it is important to study the flow statistics. Although efforts of mankind on understanding turbulence physics can be traced back to Leonardo da Vinci (1452-1519, see Fig. 1), the modern scientific approach began with the ground-breaking contribution of Osborne Reynolds (1842-1912, see Fig. 2), who conducted the famous **Reynolds experiment** (1883) and proposed first statistical approach to study turbulence (1895). As shown in Fig. 2, in the Reynolds experiment of a pipe flow, the flow starts to transition from laminar to turbulent pattern once the **Reynolds number*** reaches its critical value ($Re_D = \frac{UD}{\nu} \approx 2300$). Here, D is diameter of the pipe. The statistical approach introduced by Reynolds (1895) is the so-called "**Reynolds Averaged Navier-Stokes (RANS)**" approach, which is still one of the popular methods in turbulence study.

Interesting web links related to history of turbulence study:
Leonardo da Vinci: http://en.wikipedia.org/wiki/Da%5FVinci
Osborne Reynolds: http://en.wikipedia.org/wiki/Osborne%5FReynolds
Turbulence images: Google image with key words: turbulent flows.

*The Reynolds number is defined as

$$Re = \frac{\rho U L}{\mu} = \frac{UL}{\nu} \quad , \tag{1}$$

where, U and L are **characteristic** velocity and length scales, respectively. The meaning of the Reynolds number is that it represents the ratio of inertial forces over viscous forces:

$$Re = \frac{\rho U L}{\mu} = \frac{\rho U^2}{\mu \frac{U}{L}} = \frac{\text{Inertial forces}}{\text{Viscous forces}} \quad , \tag{2}$$

Here, the strength of inertial forces is in proportion to ρU^2, and the strength of viscous forces is in proportion to $\mu \frac{U}{L}$ (in analogy to viscous shear stress $\tau_{yx} = \mu \frac{du}{dy}$ for Newtonian fluids).

► The inertial forces are related to convection (indicated by U^2), which tend to make the flow unstable (the higher the speed U, the less stable of the flow) and facilitate turbulence.

► The viscous forces, on the opposite, tend to make the flow more stable and suppresses turbulence.

Fig. 1: An Old Man and Turbulence. Leonardo di ser Piero da Vinci (April 15, 1452 – May 2, 1519), an Italian Renaissance polymath: painter, sculptor, architect, musician, mathematician, engineer, inventor, anatomist, geologist, cartographer, botanist, and writer. Source of figure: [3].

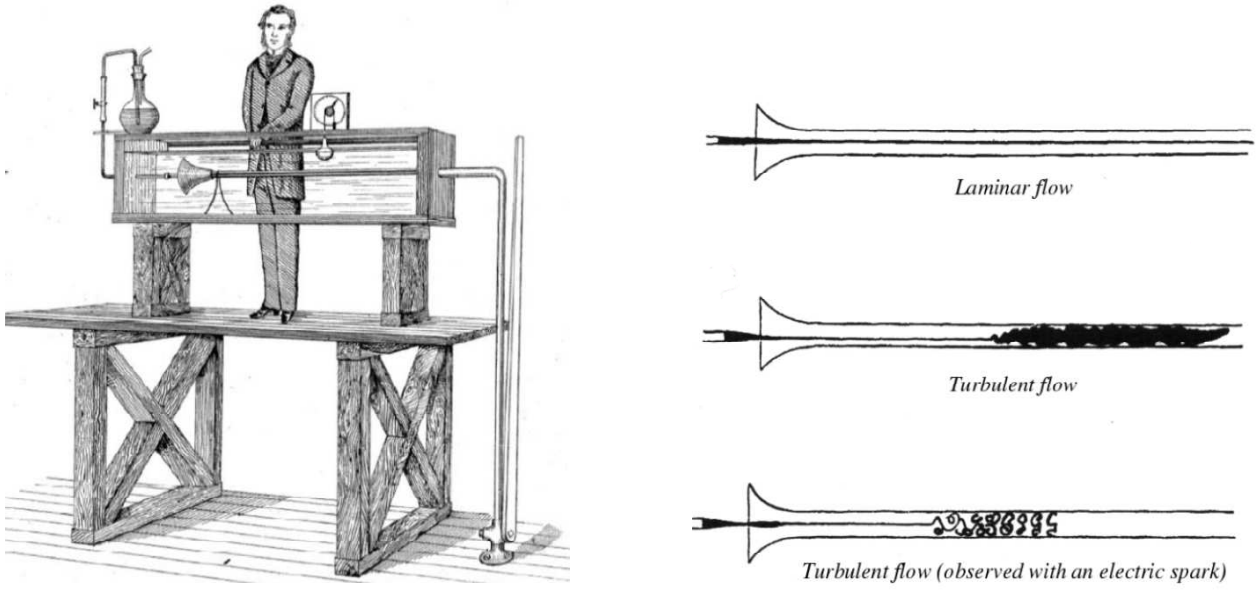

Fig. 2: Osborne Reynolds's ground-breaking experiment on laminar and turbulent flow. Osborne Reynolds (August 23, 1842 – February 21, 1912), Fellow of Royal Society, Professor of Engineering at Owens College in Manchester (now the University of Manchester). Source of figure: [4].

1.2. Reynolds Averaging and RANS

Following the approach of Reynolds (1895), Reynolds averaging can be used for extracting flow statistics from a turbulent field. The simplest approach for performing Reynolds averaging is time-averaging. A time-averaged (mean) velocity is determined as

$$\bar{u} = \lim_{T\to\infty} \frac{1}{T} \int_0^T u dt \quad . \tag{3}$$

Here, an overbar is used to indicate a time-averaged quantity. With this mean velocity, an instantaneous turbulent velocity field can be decomposed as

$$\boxed{u = \bar{u} + u'} \quad \text{(Instantaneous = Mean + Fluctuating)} \quad , \tag{4}$$

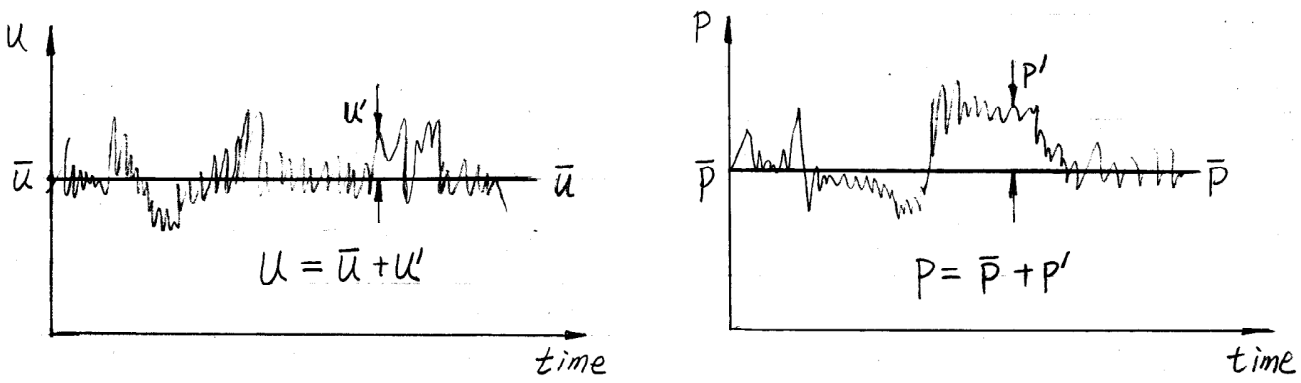

Fig. 3: Reynolds averaging for processing instantaneous turbulent velocity and pressure fields. Both $\bar{u}$ and $\bar{p}$ are constant w.r.t. time, but their values may vary w.r.t. space, i.e. $\bar{u} = \bar{u}(\mathbf{r})$ and $\bar{p} = \bar{p}(\mathbf{r})$. Here, $\mathbf{r}$ is a position vector.

where $u' = u - \bar{u}$ is the fluctuating velocity component relative to the mean velocity $\bar{u}$. The decomposition of instantaneous turbulent velocity and pressure fields are shown in Fig. 3. From the figure, it is evident that the temporally highly-fluctuating velocity and pressure, after time-averaging, become two numbers which do not vary with time (but may vary with space). In other words, both $\bar{u}$ and $\bar{p}$ are constant w.r.t. time, but their values can vary spatially (because Reynolds averaging is performed w.r.t. time instead of space).

From the definition equation for Reynolds decomposition (i.e., Eq. (4)), it is straightforward to obtain the following properties (based on two velocity components u and v):

$$\begin{aligned} &\bar{\bar{u}} = \bar{u} \quad , \\ &\overline{\bar{u}\bar{v}} = \bar{u}\bar{v} \quad , \\ &\overline{u'} = 0 \quad , \\ &\overline{\bar{u}v'} = \bar{\bar{u}}\overline{v'} = \bar{u}\overline{v'} = 0 \quad . \end{aligned} \tag{5}$$

Applying time-averaging to the product of two fluctuating velocity components u' and v', we obtain the so-called **temporal correlation** of u' and v', i.e. $\overline{u'v'}$, which is not necessarily zero. Later, this term, $\overline{u'v'}$, will be identified as a "Reynolds stress" component.

By applying Reynolds-averaging to continuity and N-S equations, the following set of two equations that governs the **mean** flow fields (i.e., $\bar{\mathbf{V}} = [\bar{u}, \bar{v}, \bar{w}]$ and $\bar{p}$) is obtained, viz.

Reynolds-Averaged Governing Equations for the Mean Flow Motion of Turbulence:

$$\begin{cases} \text{Continuity Equation:} & \nabla \cdot \bar{\mathbf{V}} = 0 \quad , \\ \text{Momentum Equation:} & \rho \dfrac{D\bar{\mathbf{V}}}{Dt} = \underbrace{-\nabla \bar{p}}_{\substack{\text{Pressure} \\ \text{gradient}}} + \underbrace{\nabla \cdot \boldsymbol{\tau}_{\text{tot}}}_{\substack{\text{Total shear} \\ \text{stresses}}} + \underbrace{\rho \mathbf{g}}_{\substack{\text{Body} \\ \text{force}}} \quad , \end{cases} \tag{6}$$

with the **total shear stress** given as

$$\boxed{\boldsymbol{\tau}_{\text{tot}} = \boldsymbol{\tau}_{\text{vis}} + \boldsymbol{\tau}_{\text{turb}}} \quad , \tag{7}$$

where $\boldsymbol{\tau}_{\text{vis}}$ is the **viscous shear stress**, and $\boldsymbol{\tau}_{\text{turb}}$ is the **turbulent shear stress**. The appearance of turbulent shear stress $\boldsymbol{\tau}_{\text{turb}}$ is due to the convection term, and $\boldsymbol{\tau}_{\text{turb}}$ is also often referred to as the **Reynolds shear stress** (or simply, Reynolds stress).

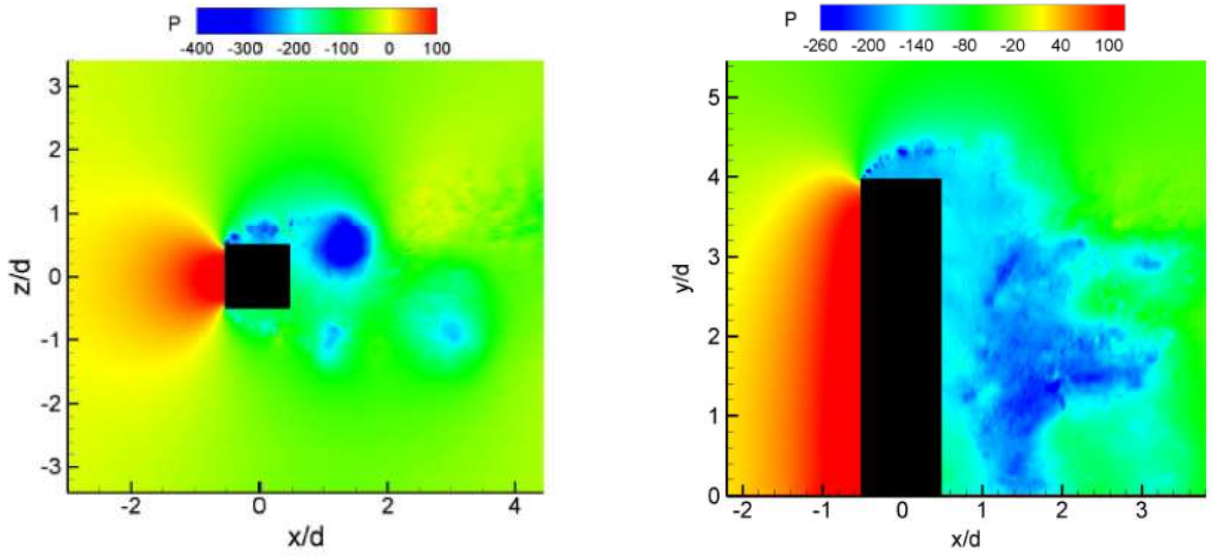

(a) Horizontal view (b) Vertical view

Fig. 4: **Instantaneous** vortex shedding pattern visualized using the instantaneous pressure for a turbulent flow past a square cylinder. The instantaneous turbulent field features irregular vortices. The instantaneous velocity field was generated using Direct Numerical Simulations conducted on supercomputers by M. Saeedi and B.-C. Wang. Click the following two links for animations:
http://home.cc.umanitoba.ca/%7Ewang44/Teaching/MECH%203492/Animations/lateral.wmv
http://home.cc.umanitoba.ca/%7Ewang44/Teaching/MECH%203492/Animations/upview.wmv

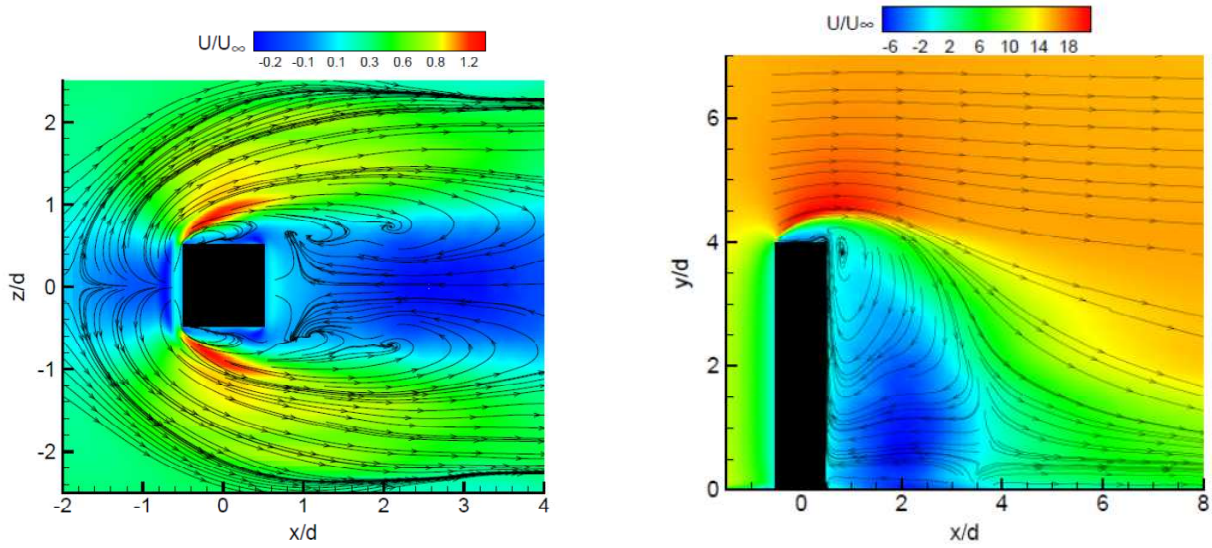

(a) Horizontal view (b) Vertical view

Fig. 5: **Time-averaged** streamlines and non-dimensionalized streamwise velocity contours for a turbulent flow past a square cylinder. The time-averaged velocity field exhibits regular-patterned pathlines, which can be interpreted as results of Reynolds averaging. Figures are made by M. Saeedi and B.-C. Wang.

To demonstrate the Reynolds averaging effects, here we compare a turbulent velocity field before and after time averaging. Figure 4 shows the vortex shedding pattern visualized using the instantaneous pressure of a turbulent flow past a square cylinder. The instantaneous turbulent field exhibits energetic and irregular vortices or eddy motions (you may click the web links given in the figure caption for

animations). However, as shown in Fig. 5, after time averaging, regular-patterned streamlines appear and the mean velocity field exhibits stable and organized flow structures. The above set of governing equation can be used for predicting the mean velocity field shown in Fig. 5.

1.3. Eddy Viscosity

The viscous shear stress has been thoroughly studied in Chapters 2 and 3. It is represented by a tensor, i.e.

$$[\boldsymbol{\tau}_{\text{vis}}] = \begin{bmatrix} \tau_{xx} & \tau_{yx} & \tau_{zx} \\ \tau_{xy} & \tau_{yy} & \tau_{zy} \\ \tau_{xz} & \tau_{yz} & \tau_{zz} \end{bmatrix} \quad . \tag{8}$$

The viscous shear stress tensor $\boldsymbol{\tau}_{\text{vis}}$ can be modelled using **Stokes' hypothesis**, which assumes that

$$\begin{aligned} &\tau_{xx} = \mu\left(\tfrac{\partial u}{\partial x} + \tfrac{\partial u}{\partial x}\right), && \tau_{yy} = \mu\left(\tfrac{\partial v}{\partial y} + \tfrac{\partial v}{\partial y}\right), && \tau_{zz} = \mu\left(\tfrac{\partial w}{\partial z} + \tfrac{\partial w}{\partial z}\right), \\ &\tau_{xy} = \tau_{yx} = \mu\left(\tfrac{\partial v}{\partial x} + \tfrac{\partial u}{\partial y}\right), && \tau_{yz} = \tau_{zy} = \mu\left(\tfrac{\partial w}{\partial y} + \tfrac{\partial v}{\partial z}\right), && \tau_{zx} = \tau_{xz} = \mu\left(\tfrac{\partial u}{\partial z} + \tfrac{\partial w}{\partial x}\right), \end{aligned} \tag{9}$$

where μ is the **dynamic viscosity** of the fluid.

Similarly, the **Reynolds shear stresses** are also represented by a tensor, which for an incompressible flow, is defined as

$$[\mathbf{R}] = [\boldsymbol{\tau}_{\text{turb}}] = \begin{bmatrix} -\rho\overline{u'u'} & -\rho\overline{u'v'} & -\rho\overline{u'w'} \\ -\rho\overline{v'u'} & -\rho\overline{v'v'} & -\rho\overline{v'w'} \\ -\rho\overline{w'u'} & -\rho\overline{w'v'} & -\rho\overline{w'w'} \end{bmatrix} \quad . \tag{10}$$

From this definition, it is understood that Reynolds shear stress components are, actually, temporal correlations between two velocity fluctuations.

In full analogy to Stokes' hypothesis for modelling $\boldsymbol{\tau}_{\text{vis}}$ (see Eq. (9)), here we have the so-called **Boussinesq's assumption** for modelling the turbulent/Reynolds shear stress tensor $\boldsymbol{\tau}_{\text{turb}}$, viz.

$$\begin{aligned} &-\rho\overline{u'u'} = \mu_t\left(\tfrac{\partial \bar{u}}{\partial x} + \tfrac{\partial \bar{u}}{\partial x}\right), && -\rho\overline{v'v'} = \mu_t\left(\tfrac{\partial \bar{v}}{\partial y} + \tfrac{\partial \bar{v}}{\partial y}\right), && -\rho\overline{w'w'} = \mu_t\left(\tfrac{\partial \bar{w}}{\partial z} + \tfrac{\partial \bar{w}}{\partial z}\right), \\ &-\rho\overline{v'u'} = -\rho\overline{u'v'} = \mu_t\left(\tfrac{\partial \bar{v}}{\partial x} + \tfrac{\partial \bar{u}}{\partial y}\right), && -\rho\overline{w'v'} = -\rho\overline{v'w'} = \mu_t\left(\tfrac{\partial \bar{w}}{\partial y} + \tfrac{\partial \bar{v}}{\partial z}\right), && -\rho\overline{w'u'} = -\rho\overline{u'w'} = \mu_t\left(\tfrac{\partial \bar{u}}{\partial z} + \tfrac{\partial \bar{w}}{\partial x}\right), \end{aligned} \tag{11}$$

where μ_t is the so-called **eddy viscosity** of turbulence. The introduction of the concept of eddy viscosity is the first step for "**turbulence modelling**", which deals with the methods for modelling the value of μ_t.

It should be indicated that unlike μ (which is a molecular property of the fluid, and can be treated as a constant at a given temperature), eddy viscosity μ_t is usually a variable w.r.t. space, i.e. $\boxed{\mu_t = \mu_t(\mathbf{r})}$. Here, $\mathbf{r} = \hat{\mathbf{i}}x + \hat{\mathbf{j}}y + \hat{\mathbf{k}}z$ is a position vector. With Eqs. (9) and (11) (i.e. with the concepts of viscosity μ and eddy viscosity μ_t), the set of governing equations represented by Eq. (6) can be further expressed as

Reynolds-Averaged Governing Equations (with Eddy Viscosity Model) for Turbulence:

$$\begin{cases} \text{Continuity Equation:} & \nabla \cdot \bar{\mathbf{V}} = 0 \quad , \\ \text{Momentum Equation:} & \rho\dfrac{D\bar{\mathbf{V}}}{Dt} = -\nabla\bar{p} + \nabla\cdot\left[(\mu+\mu_t)\nabla\bar{\mathbf{V}}\right] + \rho\mathbf{g} \quad , \end{cases} \tag{12}$$

Key features about this set of governing equations for turbulence:
• overbars for representing the mean fields (due to Reynolds averaging);
• μ is the dynamic viscosity, which is a molecular property of the fluid. Its value can be treated as a constant (at a given temperature);
• μ_t is eddy viscosity, which is not a molecular property of the fluid. Instead, it is a consequence of turbulent eddy motions and interactions. Its value varies with space (because turbulent eddies are not uniformly distributed in space), i.e. $\mu_t = \mu_t(\mathbf{r})$. In other words, μ_t represents a hypothetic concept that is invented to describe turbulent flow motions;
• The introduction of μ is due to Stokes' hypothesis for modelling $\boldsymbol{\tau}_{\text{vis}}$, and in a full analogy, the introduction of μ_t is due to Boussinesq's assumption for modelling $\boldsymbol{\tau}_{\text{turb}}$ (see, Eq. (9) and Eq. (11), respectively).
• For laminar flows, $\mu_t \equiv 0$, and then, the above governing equations reduce to those familiar forms used previously in Chapter 2 (i.e., $\rho\frac{D\bar{\mathbf{V}}}{Dt} = -\nabla\bar{p} + \mu\nabla^2\bar{\mathbf{V}} + \rho\mathbf{g}$).
• To deal with turbulence, just insert μ_t besides μ in the N-S equation (simple!).

2. Boundary-Layer Theory

2.1. Viscous Flow and Boundary Layer

In 1904, Ludwig Prandtl (February 4, 1875 – August 15, 1953), a 29-year-old German professor at the Technische Hochschule in Hanover, established the famous "boundary-layer theory" for investigating a viscous flow over a solid surface. According the Prandtl, when a viscous flow passes over a solid surface, a very thin boundary layer develops in the immediate vicinity of the solid surface where the viscous forces dominate; however, above this thin boundary layer, the flow is dominated by inertial forces (ρU^2) and can be approximately treated as inviscid.

For a viscous flow passing over a solid surface,
• within the very thin boundary layer close to the wall, the viscous force effect (or, viscous shear stress $\tau_{yx} = \mu\frac{du}{dy}$) plays a dominant role. This is because in the vicinity of the wall, the flow speed is very low (therefore, the inertial force ρU^2 is very small), but the vertical velocity gradient $\frac{du}{dy}$ is large (therefore, the viscous shear stress τ_{yx} is significant);
• above the thin boundary layer, however, the flow speed becomes much higher (therefore, the inertial force ρU^2 increases significantly), but the vertical velocity gradient $\frac{du}{dy}$ becomes much smaller (therefore, the viscous shear stress τ_{yx} decreases significantly). As such, the fluid can be approximately treated as an inviscid fluid above the boundary layer.

In the vicinity of the wall, the viscous effects are dominant, which then have two consequences:
► enforcement of no-slip boundary condition right on a solid surface, and
► creation of a thin boundary layer near the wall.

In summary, major differences between inviscid and viscous flows in the near-wall region include:
• the concepts of "viscous shear stresses", "viscous drag forces"†, "boundary layer" and "no-slip boundary condition" represent the viscous effects and are applicable to viscous flows only. These effects are absent in an inviscid flow.
• if the fluid is inviscid ($\mu \equiv 0$), there are no such concepts called viscous shear stress, viscous drag and boundary layer. Furthermore, on a solid surface, the boundary can slip (i.e., a flow may have a finite speed right on a solid surface) in an inviscid flow.

†**Viscous shear stresses** (e.g., τ_{xx}, τ_{yx}, τ_{zx} etc.) represented by Eq. (9) exist everywhere in a viscous flow, i.e. they are functions of space. The viscous shear stress acting right on a solid surface is referred to as the "**wall friction shear stress**" (or, "skin friction shear stress"), i.e. $\tau_w = \tau_{wall}$. The **viscous drag force** is defined as the integral of τ_w over a finite surface area of a finite object, i.e. $F_D = \int_A \tau_w dA$.

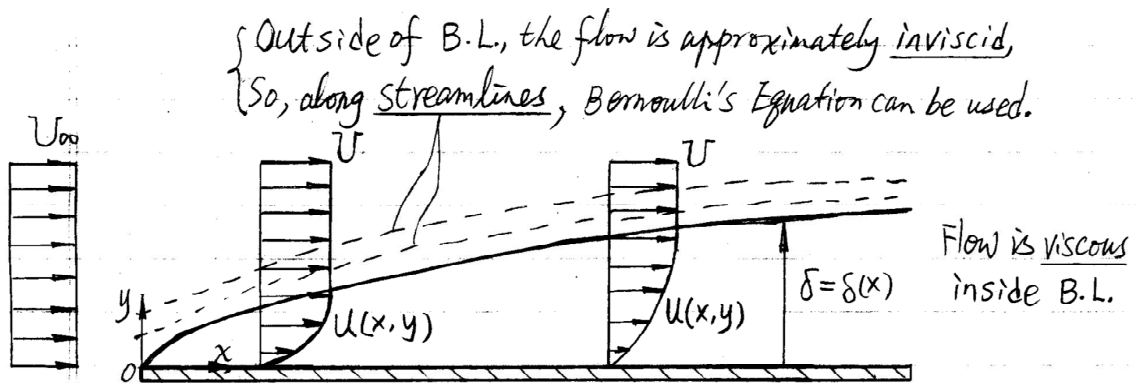

Fig. 6: A streamwise-developing laminar boundary-layer over a flat plate. Right at the inlet, the free-stream velocity is $U = U_\infty$ and hits the leading edge of the flat plate with zero incidence (i.e., parallel to the plate). Along the BL, the free-stream velocity profile above the BL is a function of x, i.e. $U = U(x)$.

2.2. Boundary-Layer Equations

Figure 6 shows a streamwise-developing laminar boundary layer after a uniform viscous flow (with inlet speed U_∞) passes a flat plate with zero incidence (i.e., parallel to the plate). In order to study the dynamics of this boundary layer, there are two approaches, i.e. differential approach and integral approach, which lead to the so-called **boundary-layer differential equations** and **boundary-layer integral equations**, respectively. In the remainder of this subsection, we study these two types boundary-layer equations.

2.2.1. Boundary-Layer Differential Equations

For a steady laminar boundary layer (BL) shown in Fig. 6, we assume that the flow is 2-D. Therefore, the BL differential equations can be derived from the general 3-D governing equations addressed in Chapter 2. Furthermore, to make the analysis simple, we consider a BL free from body forces:

$$\begin{cases} \text{Continuity Equation: } \dfrac{\partial u}{\partial x} + \dfrac{\partial v}{\partial y} = 0 \quad , \\ \text{Momentum Equation: } \begin{cases} \rho\left(u\dfrac{\partial u}{\partial x} + v\dfrac{\partial u}{\partial y}\right) = -\dfrac{\partial p}{\partial x} + \mu\left(\dfrac{\partial^2 u}{\partial x^2} + \dfrac{\partial^2 u}{\partial y^2}\right) \\ \rho\left(u\dfrac{\partial v}{\partial x} + v\dfrac{\partial v}{\partial y}\right) = -\dfrac{\partial p}{\partial y} + \mu\left(\dfrac{\partial^2 v}{\partial x^2} + \dfrac{\partial^2 v}{\partial y^2}\right) \quad . \end{cases} \end{cases} \tag{13}$$

In 1904, Prandtl introduced the boundary-layer theory based on the following **boundary-layer assumptions**:

- Inside a BL, the flow is treated viscous; but outside of the BL, the flow is treated as inviscid.
- Inside a BL, it assumed that the magnitudes of the velocities and velocity gradients follow:

$$\begin{cases} \text{Velocities:} & u \gg v \quad , \\ \text{Velocity Gradients:} & \dfrac{\partial u}{\partial y} \gg \dfrac{\partial u}{\partial x} \, , \quad \dfrac{\partial v}{\partial y} \gg \dfrac{\partial v}{\partial x} \quad , \end{cases} \tag{14}$$

Therefore, in the x-momentum equation in Eq. (13), $\frac{\partial^2 u}{\partial y^2} = \frac{\partial}{\partial y}(\frac{\partial u}{\partial y}) \gg \frac{\partial^2 u}{\partial x^2} = \frac{\partial}{\partial x}(\frac{\partial u}{\partial x})$, and it can simplified to

$$\rho\left(u\frac{\partial u}{\partial x} + v\frac{\partial u}{\partial y}\right) = -\frac{\partial p}{\partial x} + \mu\frac{\partial^2 u}{\partial y^2} \quad . \tag{15}$$

As for the y-momentum equation in Eq. (13), we have

$$\rho\Big(\underbrace{u\frac{\partial v}{\partial x}}_{\text{small}}+\underbrace{v\frac{\partial v}{\partial y}}_{\text{small}}\Big)=-\frac{\partial p}{\partial y}+\mu\Big(\underbrace{\frac{\partial^2 v}{\partial x^2}}_{\text{very small}}+\underbrace{\frac{\partial^2 v}{\partial y^2}}_{\text{small}}\Big) \quad , \tag{16}$$

which can be further simplified by neglecting the small and very small quantities to

$$\boxed{\frac{\partial p}{\partial y}=0} \quad \text{or,} \quad \boxed{p=p(x)} \text{ only.} \tag{17}$$

This equation clearly indicates that the **pressure does not change in the vertical direction in a BL**.

Differential Equations for A Steady Laminar Boundary-Layer

$$\begin{cases} \text{Continuity Equation: } \dfrac{\partial u}{\partial x}+\dfrac{\partial v}{\partial y}=0 \quad , \\ \text{Momentum Equation: } \begin{cases} \rho\Big(u\dfrac{\partial u}{\partial x}+v\dfrac{\partial u}{\partial y}\Big)=\rho U\dfrac{\partial U}{\partial x}+\mu\dfrac{\partial^2 u}{\partial y^2} \quad , \\ \dfrac{\partial p}{\partial y}=0 \quad . \end{cases} \end{cases} \tag{18}$$

The above x-momentum equation for a steady laminar BL can be also written as

$$\rho\Big(u\frac{\partial u}{\partial x}+v\frac{\partial u}{\partial y}\Big)=\rho U\frac{\partial U}{\partial x}+\frac{\partial \tau}{\partial y} \quad , \tag{19}$$

with the viscous shear stress defined as

$$\tau=\mu\frac{\partial u}{\partial y} \quad . \tag{20}$$

To derive the above BL x-momentum equation represented by Eq. (18) (or, Eq. (19)) from Eq. (15), we further used a conclusion $-\frac{dp}{dx}=\rho U\frac{dU}{dx}$. According to Prandtl's BL assumption, the flow outside of the BL can be treated as an inviscid fluid (including the edge of the BL). Therefore, using the knowledge learned from Chapter 3, for an inviscid flow, along a streamline, Bernoulli's equation can be used for determining the pressure. Furthermore, as mentioned earlier, we are analyzing a simple BL free from body forces. Therefore, right along the edge of the BL (which is a streamline), Bernoulli's equation reads

$$p+\frac{\rho U^2}{2}=C \quad . \tag{21}$$

Differentiate both sides of this equation w.r.t. x to obtain

$$\frac{dp}{dx}+\rho U\frac{dU}{dx}=0 \quad , \tag{22}$$

or,

$$\boxed{-\frac{dp}{dx}=\rho U\frac{dU}{dx}} \quad . \tag{23}$$

Because within a BL, $\partial p/\partial y\equiv 0$ (see Eq. (20)), it is now clear that p only changes with x, and dp/dx is the only pressure gradient component within a BL. This equation indicates that the pressure gradient

dp/dx inside a BL can be figured out using the free-stream velocity U above the BL. As shown in Fig. 6, right at the inlet, the free-stream velocity is $U = U_\infty$. Along the BL, the free-stream above the BL is treated as an inviscid fluid and its velocity profile is a function of x only, i.e. $\boxed{U = U(x)}$.

► From Eq. (23), it is understood that the only reason that the free-stream velocity U changes w.r.t. x is because of the pressure gradient $\frac{dp}{dx}$.

► For a zero pressure gradient (ZPG) boundary layer, $\frac{dp}{dx} \equiv 0$, and therefore, $U = U(x) \equiv U_\infty$. The reason that U does not change along the streamline in a ZPG BL is because the free-stream above the BL is treated as an inviscid fluid according to Prandtl's BL theory, and as a result, there is no head loss in the free-stream above the BL.

► Within the BL, the flow is treated as a viscous fluid, and of course, viscous shear stresses exist and cause head losses. The velocity profile u within a BL varies with x and y, i.e. $\boxed{u = u(x, y)}$.

2.2.2. Boundary-Layer Thickness and Integral Parameters

(1) Boundary-Layer Thickness

As shown in Fig. 6, the BL thickness keeps growing (monotonically) along the plate, and is a function of the streamwise distance, i.e. $\boxed{\delta = \delta(x)}$. The velocity profile $u = u(x, y)$ is zero at the wall and keeps increasing in value as the elevation increases (i.e., as y increases). Right at the outer-edge of the boundary-layer (at elevation $y = \delta$), u approaches the free-stream velocity, i.e. $u = U$. However, in order for u to reach U asymptotically, the BL thickness δ can be very large in some cases. Therefore, in practice, we often use an **alternative BL thickness** definition, which specifies the outer-edge of a BL as the vertical position where

$$u = 0.99U \quad . \tag{24}$$

We denote this alternative BL thickness as "δ_{99}".

(2) Displacement Thickness

Figure 7 shows a streamwise developing BL over a flat plate. Between the plate and the streamline shown in the figure, the mass flow rate (per unit depth) is constant, meaning that the mass flow rate at inlet ($x = 0$) is equal to the that at the outlet ($x = L$), i.e.

$$\rho U h = \int_0^\delta \rho u dy + \rho U (h' - \delta) \quad , \tag{25}$$

which can be further rearranged to

$$\rho U (h' - h) = \rho U \delta - \int_0^\delta \rho u dy = \int_0^\delta \rho (U - u) dy \quad . \tag{26}$$

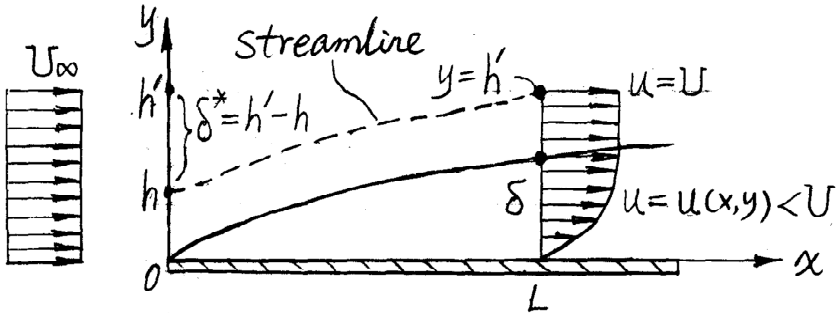

Fig. 7: Schematic demonstration of the cause of the displacement thickness (δ^*) of a boundary layer.

Define the **displacement thickness** as

$$\delta^* = h' - h \quad , \tag{27}$$

then we obtain

$$\rho U \delta^* = \int_0^\delta \rho(U-u)dy \quad , \tag{28}$$

or,

$$\boxed{\delta^* = \int_0^\delta \left(1 - \frac{u}{U}\right) dy} \quad . \tag{29}$$

If $y \geq \delta$, $u \equiv U$ and $1 - \frac{u}{U} = 0$. Therefore, we can also express displacement thickness δ^* as

$$\boxed{\delta^* = \int_0^\infty \left(1 - \frac{u}{U}\right) dy} = \int_0^\delta \left(1 - \frac{u}{U}\right) dy + \cancelto{0}{\int_\delta^\infty \left(1 - \frac{u}{U}\right) dy} \, . \tag{30}$$

Physical Meaning:

• Because of the existence of the BL, the velocity u is smaller than the free-stream velocity U. This is to say, as shown in Fig. 7, the streamline needs to be *pushed out* (or, "*displaced*") vertically from position h to position h' in order to maintain mass conservation.

• The concept of displacement thickness is purely due to the requirement of mass conservation.

• The difference between h and h' is exactly the displacement thickness, i.e. $\delta^* = h' - h$ (see Fig. 7).

(3) Momentum Thickness

Figure 8 analyzes the momentum balance over a finite control volume ABCD in the context of a streamwise developing BL over a flat plate. The x-momentum fluxes (per unit depth) across the boundary (4 sides) of the control volumes are shown in the figure, viz.

$$\begin{aligned}
&\text{across side AB:} \quad M_{AB} = \int_0^\infty \rho U^2 dy \quad , \\
&\text{across side BC:} \quad M_{BC} = U \cdot \int_0^\infty \rho(U-u)dy \quad , \\
&\text{across side CD:} \quad M_{CD} = \int_0^\infty \rho u^2 dy \quad , \\
&\text{across side DA:} \quad M_{DA} = 0 \quad .
\end{aligned} \tag{31}$$

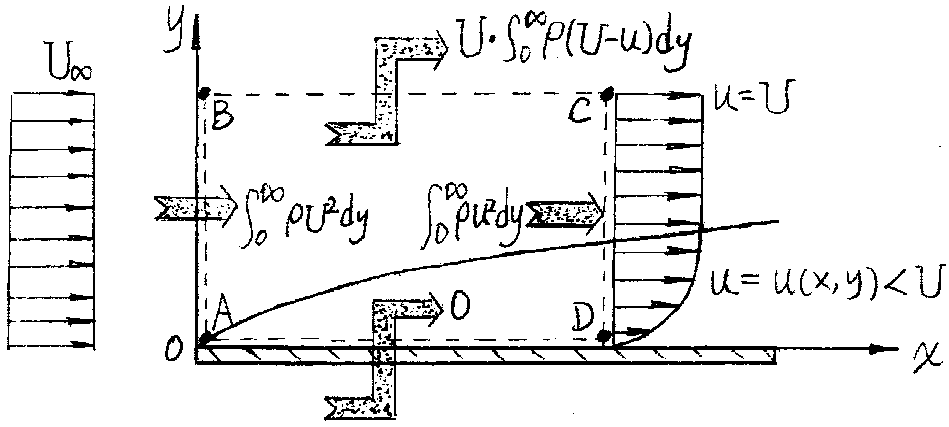

Fig. 8: Schematic demonstration of the cause of the momentum thickness (θ) of a boundary layer.

The explanation of the above equations is straightforward.[‡] The net rate of loss in the x-momentum (per unit depth) for an incompressible viscous flow over the control volume is, therefore,

$$\begin{aligned}\text{Momentum Loss} &= M_{AB} - M_{BC} - M_{CD} \\ &= \int_0^\infty \rho U^2 dy - U \cdot \int_0^\infty \rho(U-u)dy - \int_0^\infty \rho u^2 dy \\ &= \int_0^\infty \rho\left[U^2 - U(U-u) - u^2\right] dy \\ &= \rho \int_0^\infty u(U-u)dy \quad .\end{aligned} \tag{34}$$

Define parameter θ such that

$$\rho U^2 \theta = \text{Momentum Loss} = \rho \int_0^\infty u(U-u)dy \quad , \tag{35}$$

which can be further rearranged to

$$\boxed{\theta = \int_0^\infty \frac{u}{U}\left(1 - \frac{u}{U}\right) dy} \quad , \tag{36}$$

which is referred to as the **momentum thickness** of a BL. Because $u \equiv U$ if $y \geq \delta$, the integrand is essentially zero for $y \geq \delta$, resulting in: $\int_\delta^\infty \frac{u}{U}\left(1 - \frac{u}{U}\right) dy = 0$. Therefore, we can also express momentum thickness θ as

$$\boxed{\theta = \int_0^\delta \frac{u}{U}\left(1 - \frac{u}{U}\right) dy} \quad . \tag{37}$$

Physical Meaning:

- Because of the existence of the BL, momentum decreases as the viscous fluid flows downstream.
- The momentum thickness θ describes the momentum loss due to the existence of BL.
- The "amount" of momentum loss equals to the momentum carried by a flow layer with thickness θ at the inlet (before the BL starts to develop, where the free stream velocity is U).

[‡]The velocity is uniform and constant at the inlet (AB), viz. $u = U$; but because of the existence of the BL, $u = u(x, y)$ is a variable at outlet (CD). The mass flow rates (per unit depth) across AB and CD are

$$m_{_{AB}} = \int_0^\infty \rho U dy \quad \text{and} \quad m_{_{CD}} = \int_0^\infty \rho u dy \quad , \tag{32}$$

respectively. There is no mass flow across of the solid plate surface (DA), i.e. $m_{_{DA}} = 0$. Therefore, the balance between the mass flow rates at the inlet (AB) and outlet (CD) has to go across the top boundary (BC), i.e.

$$m_{_{BC}} = \int_0^\infty \rho U dy - \int_0^\infty \rho u dy = \int_0^\infty \rho(U-u)dy \quad . \tag{33}$$

At BC, the velocity is U, therefore, the momentum across BC is $M_{BC} = m_{_{BC}} \cdot U = U \cdot \int_0^\infty \rho(U-u)dy$.

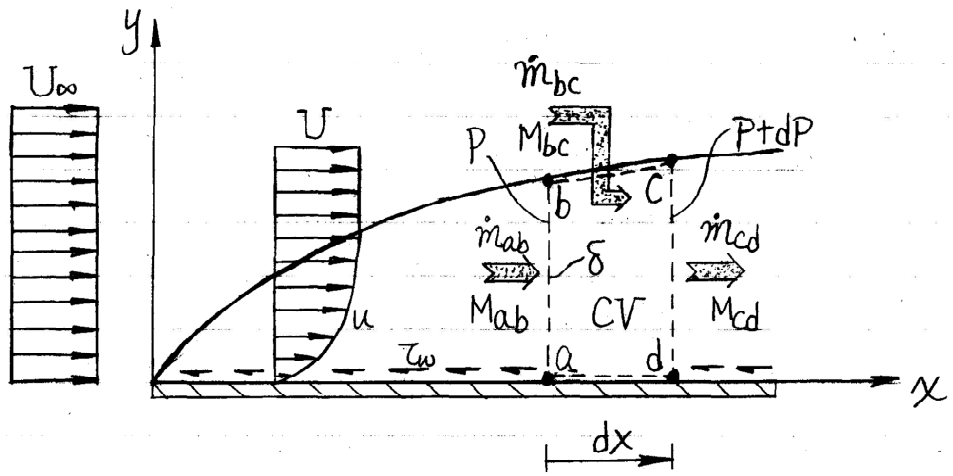

Fig. 9: Analysis of mass and momentum balance over a control volume (of a finite-height from 0 to δ) a-b-c-d in a boundary layer. Streamwise, the wall friction shear stress is τ_w, and over the control volume (dx), the pressure increases from p to $p + dp$.

2.2.3. Boundary-Layer Momentum Integral Equation (pp. 428-433)

In subsection 2.2.1, the BL differential equations (i.e., Eq. (18)) have introduced, which govern the BL flow motion from a differential (local and infinitesimal) point of view. In this subsection, we introduce the BL integral equation, which study the momentum balance of the BL flow from an integral point of view over a finite BL height δ.

(1) Mass Balance

Figure 9 shows the mass balance over a control volume (CV) a-b-c-d. The mass flow rates (per unit depth) across each sides are:

$$\begin{aligned}
&\text{across side ab:} \quad \dot{m}_{ab} = \dot{m}_x = \int_0^\delta \rho u dy \quad , \\
&\text{across side cd:} \quad \dot{m}_{cd} = \dot{m}_{ab} + \frac{d\dot{m}_x}{dx} dx = \dot{m}_{ab} + \frac{d}{dx}\left(\int_0^\delta \rho u dy\right) dx \quad , \\
&\text{across side da:} \quad \dot{m}_{da} = 0 \quad .
\end{aligned} \tag{38}$$

Due to mass conservation, the mass flow rate across side bc is

$$\text{across side bc:} \quad \dot{m}_{bc} = \dot{m}_{cd} - \dot{m}_{ab} = \frac{d}{dx}\left(\int_0^\delta \rho u dy\right) dx \quad . \tag{39}$$

(2) Momentum Balance (BL Integral Equation)

Similar to the mass balance analysis presented above, as shown Fig. 9, the x-momentum (per unit depth) across the four sides of the control volume are:

$$\begin{aligned}
&\text{across side ab:} \quad M_{ab} = M_x = \int_0^\delta \rho u^2 dy \quad , \\
&\text{across side bc:} \quad M_{bc} = \dot{m}_{bc} \cdot U = U \cdot \frac{d}{dx}\left(\int_0^\delta \rho u dy\right) dx \quad \text{(based on Eq. (39))}, \\
&\text{across side cd:} \quad M_{cd} = M_{ab} + \frac{dM_x}{dx} dx = M_{ab} + \frac{d}{dx}\left(\int_0^\delta \rho u^2 dy\right) dx \quad , \\
&\text{across side da:} \quad M_{da} = 0 \quad .
\end{aligned} \tag{40}$$

According to Newton's second law, the x-momentum change is due to the two external forces (per unit depth), i.e. the streamwise pressure forces and the wall friction forces. As shown in Fig. 9, the net pressure forces is $[(p+dp)-p]\cdot\delta = dp\cdot\delta$, and wall friction forces is $\tau_w \cdot dx$. The x-momentum balances as

$$\begin{aligned}\overbrace{-dp\cdot\delta-\tau_w\cdot dx}^{\text{External forces}} = \overbrace{\sum M_{out}-\sum M_{in}}^{\text{Momentum change}} &= M_{cd}-M_{ab}-M_{bc}-\cancelto{0}{M_{da}} \\ &= \left[\cancel{M_{ab}}+\frac{\partial}{\partial x}\left(\int_0^\infty \rho u^2 dy\right)dx\right]-\cancel{M_{ab}}-M_{bc} \\ &= \frac{d}{dx}\left(\int_0^\delta \rho u^2 dy\right)dx - U\cdot\frac{d}{dx}\left(\int_0^\delta \rho u dy\right)dx \quad .\end{aligned} \tag{41}$$

or,

$$-\frac{dp}{dx}\delta-\tau_w = \frac{d}{dx}\left(\int_0^\delta \rho u^2 dy\right) - U\cdot\frac{d}{dx}\left(\int_0^\delta \rho u dy\right) \quad . \tag{42}$$

From Eq. (23), it is understood that the streamwise pressure gradient within the entire BL follows $-\frac{dp}{dx}=\rho U\frac{dU}{dx}$. Also, we recognize that $\delta=\int_0^\delta dy$. Therefore, the above x-momentum balance equation can be further expressed as

$$\rho U\frac{dU}{dx}\int_0^\delta dy-\tau_w = \frac{d}{dx}\left(\int_0^\delta \rho u^2 dy\right)dx - U\cdot\frac{d}{dx}\left(\int_0^\delta \rho u dy\right) \quad . \tag{43}$$

Because the free-stream velocity $U=U(x)$ (which does not vary with y), we further obtain

$$\tau_w = \frac{dU}{dx}\int_0^\delta \rho U dy - \frac{d}{dx}\left(\int_0^\delta \rho u^2 dy\right) + U\cdot\frac{d}{dx}\left(\int_0^\delta \rho u dy\right) \quad . \tag{44}$$

Because of the product rule of calculus,[§] the last term in the above equation can be expressed as

$$\begin{aligned}U\cdot\frac{d}{dx}\left(\int_0^\delta \rho u dy\right) &= \frac{d}{dx}\left[U\cdot\left(\int_0^\delta \rho u dy\right)\right] - \frac{dU}{dx}\cdot\left(\int_0^\delta \rho u dy\right) \\ &= \frac{d}{dx}\left(\int_0^\delta \rho U u dy\right) - \frac{dU}{dx}\int_0^\delta \rho u dy \quad ,\end{aligned} \tag{46}$$

with which, Eq. (44) can be rearranged to

$$\tau_w = \frac{dU}{dx}\int_0^\delta \rho U dy - \frac{d}{dx}\left(\int_0^\delta \rho u^2 dy\right) + \frac{d}{dx}\left(\int_0^\delta \rho U u dy\right) - \frac{dU}{dx}\int_0^\delta \rho u dy \quad , \tag{47}$$

or,

$$\frac{\tau_w}{\rho} = \frac{d}{dx}\left[\int_0^\delta u(U-u)dy\right] + \frac{dU}{dx}\int_0^\delta (U-u)dy \quad , \tag{48}$$

and further as

$$\frac{\tau_w}{\rho} = \frac{d}{dx}\left[U^2\int_0^\delta \frac{u}{U}\left(1-\frac{u}{U}\right)dy\right] + U\frac{dU}{dx}\int_0^\delta \left(1-\frac{u}{U}\right)dy \quad . \tag{49}$$

[§]In calculus, the **product rule for differentiation** follows:

$$\frac{d}{dx}(f\cdot g) = f\cdot\frac{dg}{dx}+g\cdot\frac{df}{dx} \quad \text{or,} \quad f\cdot\frac{dg}{dx} = \frac{d}{dx}(f\cdot g)-g\cdot\frac{df}{dx} \quad . \tag{45}$$

In this special case, $f=U$ and $g=\int_0^\delta \rho u dy$.

Considering the definition of displacement thickness δ^* and momentum thickness θ of a BL (defined by Eq. (29) and Eq. (36), respectively), the above equation becomes

$$\boxed{\frac{\tau_w}{\rho} = \frac{d}{dx}\left(U^2\theta\right) + \delta^* U\frac{dU}{dx}} \quad . \tag{50}$$

which is the so-called **BL momentum integral equation**. It is also often referred to as the **Kármán integral equation**, in honor of Theodore von Kármán (1881-1963), a Hungarian-American mathematician, aerospace engineer and physicist (von Kármán obtained his Ph.D. degree under the supervision of Ludwig Prandtl at the Univ. of Göttingen in 1908, see http://en.wikipedia.org/wiki/Von%20Karman). This equation reflects overall momentum balance over a finite BL height, i.e. how the momentum of the fluid changes in the streamwise direction after being integrated vertically over BL thickness δ. The **physical meaning** of this equation is clear: the momentum loss ($\frac{d}{dx}\left(U^2\theta\right)$) is caused by the balance from the wall friction shear stress ($\frac{\tau_w}{\rho}$) and the streamwise pressure driving force ($\delta^* U\frac{dU}{dx}$, recall that $-\frac{dp}{dx} = \rho U\frac{dU}{dx}$).

The BL momentum integral equation represented by Eq. (50) can be rearranged to

$$\frac{\tau_w}{\rho} = U^2\frac{d\theta}{dx} + 2\theta U\frac{dU}{dx} + \delta^* U\frac{dU}{dx} \quad , \tag{51}$$

or,

$$\boxed{\frac{C_f}{2} = \frac{d\theta}{dx} + (2+H)\frac{\theta}{U}\frac{dU}{dx}} \quad , \tag{52}$$

where C_f is the **local skin friction coefficient** defined as

$$\boxed{C_f = \frac{\tau_w}{\frac{1}{2}\rho U^2}} \quad , \tag{53}$$

and H is the **shape factor** defined as the ratio between the displacement and momentum thicknesses:

$$\boxed{H = \frac{\delta^*}{\theta}} \quad . \tag{54}$$

2.2.4. Application of the BL Momentum Integral Equation with Zero-Pressure-Gradient (pp. 433-438)

As shown previously in Eq. (18), in a BL, the y-momentum equation degenerates to $\frac{\partial p}{\partial y} = 0$. This means that in a BL, pressure p does not vary in the y direction but may still change in the x direction (i.e., $\frac{\partial p}{\partial x}$ can be non-zero). In this subsection, we study a special case so-called **zero-pressure gradient BL** (ZPG), which further demands that $\frac{\partial p}{\partial x} = 0$. Therefore, in a ZPG BL, $\frac{\partial p}{\partial x} = 0$ and $\frac{\partial p}{\partial y} = 0$. An example of a ZPG is a flow over a flat plate, whose free-stream velocity U and pressure p are both constant (before and outside of the BL), i.e. $U \equiv U_\infty$ and $p = p_\infty$.

(1) Local Wall Friction Stress τ_w and Friction Coefficient C_f

From Eq. (23), it is understood that in a ZPG BL flow, $-\frac{dp}{dx} = \rho U\frac{dU}{dx} = 0$ or $\frac{dU}{dx} = 0$. The BL momentum integral equation represented by Eq. (51) can be, therefore, simplified to

$$\boxed{\frac{\tau_w}{\rho} = U^2\frac{d\theta}{dx}} \quad , \tag{55}$$

which can be further rearranged to

$$\boxed{\frac{C_f}{2} = \frac{d\theta}{dx}} \quad . \tag{56}$$

Substituting the definition of the momentum thickness into Eq. (55), we obtain

$$\tau_w = \rho U^2 \frac{d\theta}{dx} = \rho U^2 \frac{d}{dx} \int_0^\delta \frac{u}{U} \left(1 - \frac{u}{U}\right) dy \quad . \tag{57}$$

Define non-dimensional vertical coordinate

$$\boxed{\eta = \frac{y}{\delta}} \quad , \tag{58}$$

we get $dy = \delta d\eta$, and the momentum integral equation for a ZPG BL represented by Eq. (57) becomes

$$\tau_w = \rho U^2 \frac{d\theta}{dx} = \rho U^2 \frac{d\delta}{dx} \int_0^1 \frac{u}{U} \left(1 - \frac{u}{U}\right) d\eta \quad . \tag{59}$$

(2) General Velocity Profile and Boundary Conditions

In order to determine, e.g. τ_w, using Eq. (59), it is necessary to specify the profile for $\frac{u}{U}$. We assume the velocity profile of the BL flow, after being non-dimensionalized, is self-similar and takes the following general functional form:

$$\frac{u}{U} = f\left(\frac{y}{\delta}\right) = f(\eta) \quad . \tag{60}$$

The boundary conditions for a BL flow are

$$\text{Boundary conditions:} \begin{cases} \text{at } y = 0: & u = 0 & \text{(Dirichlet B.C.)} & , \\ \text{at } y = \delta: & u = U & \text{(Dirichlet B.C.)} & , \\ \text{at } y = \delta: & \dfrac{\partial u}{\partial y} = 0 & \text{(Neumann B.C.)} & . \end{cases} \tag{61}$$

(3) A Solution for a Laminar ZPG BL

• **Step 1** Determine the velocity profile:

As shown in Eq. (61), there are three boundary conditions for a BL flow. Therefore, we can assign maximum three degrees of freedom to a BL velocity profile. Following von Kármán, one of the possibilities is to assume that the velocity profile is a polynomial of y, i.e.

$$u = a + by + cy^2 \quad . \tag{62}$$

By applying the three boundary conditions (given in Eq. (61)) to the above velocity profile, the three coefficients can be determined, viz.

$$a = 0 \, , \quad b = 2\frac{U}{\delta} \, , \quad c = -\frac{U}{\delta^2} \quad . \tag{63}$$

The velocity can then be expressed as

$$u = 2\frac{U}{\delta} y - \frac{U}{\delta^2} y^2 \quad , \tag{64}$$

or, in a non-dimensional form as

$$\frac{u}{U} = 2\frac{y}{\delta} - \left(\frac{y}{\delta}\right)^2 = 2\eta - \eta^2 \quad . \tag{65}$$

• **Step 2** Determine the wall friction shear stress:
Once the velocity profile is obtained, we can calculate the wall friction shear stress τ_w. The calculation of τ_w can be based on the dimensional velocity profile (i.e., Eq. (64)), or the non-dimensional velocity profile (i.e., Eq. (65)). The following calculation of τ_w is based on the non-dimensional velocity profile

$$\tau_w = \mu \frac{\partial u}{\partial y}\bigg|_{y=0} = \mu \frac{U \partial (u/U)}{\delta \partial (y/\delta)}\bigg|_{y/\delta=0} = \frac{\mu U}{\delta} \frac{d(u/U)}{d\eta}\bigg|_{\eta=0} \quad , \tag{66}$$

By substituting Eq. (65) into the above equation, we obtain

$$\tau_w = \frac{\mu U}{\delta} \frac{d}{d\eta}(2\eta - \eta^2)\bigg|_{\eta=0} = \frac{\mu U}{\delta}(2-2\eta)\bigg|_{\eta=0} = \frac{2\mu U}{\delta} \quad . \tag{67}$$

• **Step 3** Determine the BL thickness δ:
Substituting the results of τ_w and $\frac{u}{U}$ (i.e., Eqs. (67) and (65), respectively) into the momentum integral equation for a ZPG BL (i.e., Eq. (59)), we obtain

$$\begin{aligned} \frac{2\mu U}{\delta} &= \rho U^2 \frac{d\delta}{dx} \int_0^1 \frac{u}{U}\left(1 - \frac{u}{U}\right) d\eta \\ &= \rho U^2 \frac{d\delta}{dx} \int_0^1 (2\eta - \eta^2)\left[1 - (2\eta - \eta^2)\right] d\eta \end{aligned} \tag{68}$$

or,

$$\frac{2\mu U}{\delta} = \rho U^2 \frac{d\delta}{dx} \int_0^1 (2\eta - 5\eta^2 + 4\eta^3 - \eta^4) d\eta \quad . \tag{69}$$

Integrating and substituting the limits yields

$$\frac{2\mu U}{\delta} = \rho U^2 \frac{d\delta}{dx} \frac{2}{15} \quad . \tag{70}$$

or,

$$\delta d\delta = \frac{15\mu}{\rho U} dx \quad , \tag{71}$$

which is an ordinary differential equation for δ. Integrating again gives

$$\frac{\delta^2}{2} = \frac{15\mu}{\rho U} x + C \quad , \tag{72}$$

Assuming that the boundary layer starts at the leading edge of the flat plate, i.e. $\delta = 0$ at $x = 0$, then we have $C = 0$. Thus,

$$\delta = \sqrt{\frac{30\mu x}{\rho U}} \quad . \tag{73}$$

This result shows that the laminar BL thickness grows as $\sqrt{x}$, i.e. it has a parabolic shape. Define Reynolds number as

$$\boxed{Re_x = \frac{\rho U x}{\mu}} \quad , \tag{74}$$

and this result (i.e., Eq. (73)) can be further expressed as

$$\frac{\delta}{x} = \sqrt{\frac{30\mu}{\rho U x}} = \boxed{\frac{5.48}{\sqrt{Re_x}}} \qquad \text{(approximate solution)} \quad . \tag{75}$$

• **Step 4** Determine the local skin friction coefficient C_f:
From the definition of C_f, we have

$$C_f = \frac{\tau_w}{\frac{1}{2}\rho U^2} = \frac{2\mu U/\delta}{\frac{1}{2}\rho U^2} = \frac{4\mu}{\rho U\delta} = 4\frac{\mu}{\rho U x}\frac{x}{\delta} = 4\frac{1}{Re_x}\frac{\sqrt{Re_x}}{5.48} \quad , \tag{76}$$

or,

$$\boxed{C_f = \frac{0.730}{\sqrt{Re_x}}} \quad \text{(approximate solution)} \quad . \tag{77}$$

The above solutions for $\frac{\delta}{x}$ and C_f (given by Eq. (75) and Eq. (76), respectively) are **approximate solutions** obtained based on the crude assumption that the velocity profile is a special quadratic polynomial of y (cf. Eq. (62)). However, this approximate result is very close to (only 10% higher than) the following **exact solution** to the BL momentum equation

$$\boxed{C_f = \frac{0.664}{\sqrt{Re_x}}} \quad \text{(exact solution)} \quad . \tag{78}$$

Without giving detailed derivations, this exact solution was first developed by Paul R. H. Blasius (1883-1970) in 1908, professor of Ingenieurschule Hamburg, Germany. Blasius was one of the first Ph.D. students of Ludwig Prandtl (see, http://en.wikipedia.org/wiki/Paul%20Richard%20Heinrich%20Blasius). Also, in the exact solution of Blasius, constant '5.48' in Eq. (75) needs to be replaced with '5.0', such that $\boxed{\frac{\delta}{x} = \frac{5.0}{\sqrt{Re_x}}}$.

In comparison with Blasius's exact solution, it is understood that our approximate solution represented by Eq. (77) depends on the assumption of the non-dimensional velocity profile $\frac{u}{U}$ for the laminar BL flow. Table 9.2 (from the textbook) well-summarizes the approximate solutions based on different assumptions on the polynomial profiles of the non-dimensional velocity $\frac{u}{U}$.

Table 9.2

Results of the Calculation of Laminar Boundary-Layer Flow over a Flat Plate at Zero Incidence Based on Approximate Velocity Profiles

Velocity Distribution $\frac{u}{U} = f\left(\frac{y}{\delta}\right) = f(\eta)$	$\beta \equiv \frac{\theta}{\delta}$	$\frac{\delta^*}{\delta}$	$H \equiv \frac{\delta^*}{\theta}$	Constant a in $\frac{\delta}{x} = \frac{a}{\sqrt{Re_x}}$	Constant b in $C_f = \frac{b}{\sqrt{Re_x}}$
$f(\eta) = \eta$	$\frac{1}{6}$	$\frac{1}{2}$	3.00	3.46	0.577
$f(\eta) = 2\eta - \eta^2$	$\frac{2}{15}$	$\frac{1}{3}$	2.50	5.48	0.730
$f(\eta) = \frac{3}{2}\eta - \frac{1}{2}\eta^3$	$\frac{39}{280}$	$\frac{3}{8}$	2.69	4.64	0.647
$f(\eta) = 2\eta - 2\eta^3 + \eta^4$	$\frac{37}{315}$	$\frac{3}{10}$	2.55	5.84	0.685
$f(\eta) = \sin\left(\frac{\pi}{2}\eta\right)$	$\frac{4-\pi}{2\pi}$	$\frac{\pi-2}{\pi}$	2.66	4.80	0.654
Exact	0.133	0.344	2.59	5.00	0.664

• **Step 5** Shape factor:
Table 9.2 includes other parameters such as the displacement thickness δ^*, momentum thickness θ and shape factor H. Here we continue our solution based on the special quadratic polynomial of y (cf. Eq. (62)) by determining these parameters.
Displacement thickness δ^*:

$$\begin{aligned}\delta^* = \int_0^\delta \left(1 - \frac{u}{U}\right) dy &= \delta \int_0^1 \left(1 - \frac{u}{U}\right) d\eta \\ &= \delta \int_0^1 \left[1 - (2\eta - \eta^2)\right] d\eta \\ &= \frac{1}{3}\delta \quad ,\end{aligned} \tag{79}$$

or, $\boxed{\frac{\delta^*}{\delta} = \frac{1}{3}}$. Once the BL thickness δ is known, the displacement thickness δ^* can be calculated accordingly. Specifically, from Eq. (75),

$$\frac{\delta^*}{x} = \frac{1}{3}\frac{5.48}{\sqrt{Re_x}} = \frac{1.83}{\sqrt{Re_x}} \quad . \tag{80}$$

Momentum thickness θ:

$$\begin{aligned}\theta = \int_0^\delta \frac{u}{U}\left(1 - \frac{u}{U}\right) dy &= \delta \int_0^1 \frac{u}{U}\left(1 - \frac{u}{U}\right) d\eta \\ &= \delta \int_0^1 (2\eta - \eta^2)\left[1 - (2\eta - \eta^2)\right] d\eta \\ &= \frac{2}{15}\delta \quad ,\end{aligned} \tag{81}$$

or, $\boxed{\frac{\theta}{\delta} = \frac{2}{15}}$. From Eq. (75), we further obtain

$$\frac{\theta}{x} = \frac{2}{15}\frac{5.48}{\sqrt{Re_x}} = \frac{0.73}{\sqrt{Re_x}} \quad . \tag{82}$$

From Eqs. (79) and (81), it is understood that for the assumed polynomial laminar BL flow (cf. Eq. (62)),

$$\delta > \delta^* > \theta \quad . \tag{83}$$

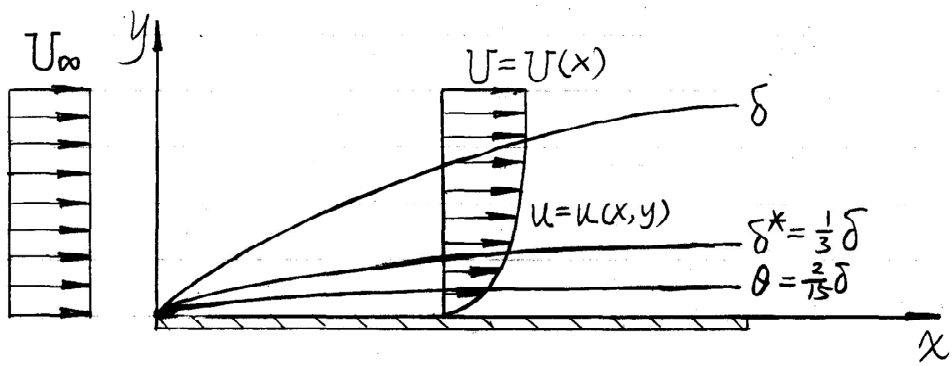

Fig. 10: Comparison of the BL thickness δ, displacement thickness δ^* and momentum thickness θ calculated using the BL integral equation based on the assumed polynomial laminar BL velocity profile given by Eq. (62), i.e. $u = a + by + cy^2$.

The relationship between these three thicknesses of the BL is shown in Fig. 10.
Shape factor H:

$$H = \frac{\delta^*}{\theta} = \left(\frac{1}{3}\delta\right) \Big/ \left(\frac{2}{15}\delta\right) = \frac{5}{2} = 2.5 \quad . \tag{84}$$

2.3. Laminar-to-Turbulent Transition BL over a Smooth Flat Plate

Thus far, we have focused our discussion on laminar BLs. As shown in Fig. 11, when flow passes over a flat plate, a laminar BL starts from the leading edge and its thickness $\delta = \delta(x)$ keeps growing in the streamwise direction (as x increases). The Reynolds number $Re_x = \frac{\rho U x}{\mu}$ also increases as x increases. As the BL grows, it becomes less stable. The exact Reynolds number at which the BL flow transitions from laminar to turbulent pattern depends on many parameters such as surface roughness, disturbances and pressure gradient. In literature, the **critical Reynolds number** for transition is about $Re_x = 5 \times 10^5 \sim 3 \times 10^6$ for a BL developed over a smooth flat plate. The upper limit on Re_x for a BL flow past over a smooth flat plate to remain laminar is 3×10^6.

In summary, a BL flow over a flat plate experiences three stages of development in the streamwise direction: laminar BL, transition BL and turbulent BL.

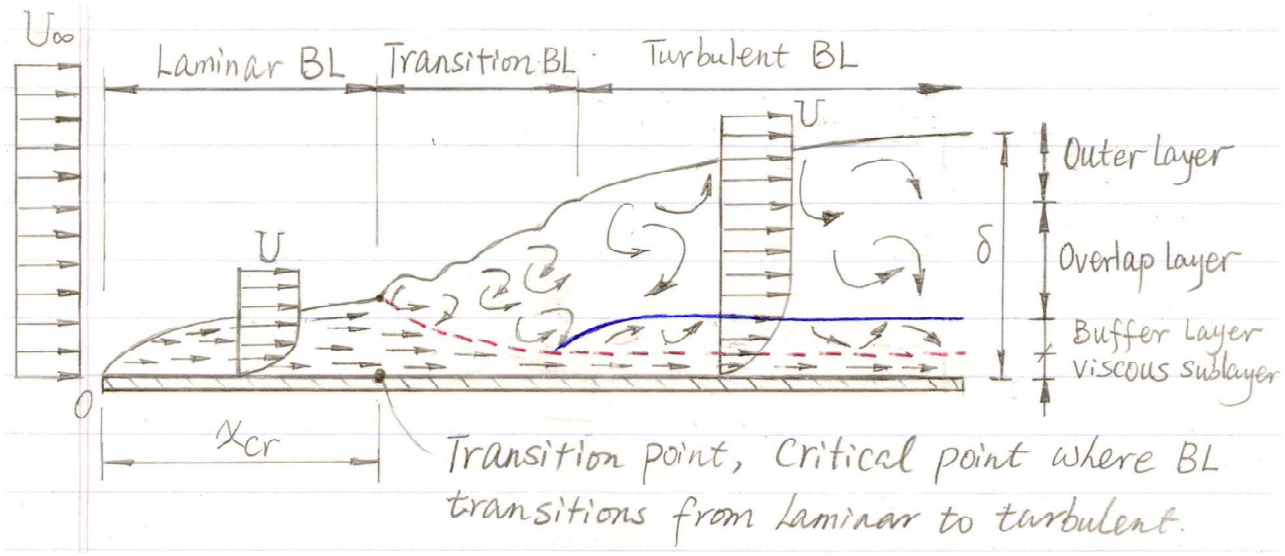

Fig. 11: Structure of a streamwise developing boundary layer over a flat plate, which transitions from a laminar to a turbulent boundary layer.

2.4. Fully-Turbulent BL

In the previous sections, we have thoroughly studied the behaviour of laminar BLs. Study of the transition BL involves knowledge on not only viscous fluid dynamics but also stability theory, which is beyond the scope of this class. Here in this subsection, we focus our attention solely on the turbulent BL (i.e., here we only study the **fully-turbulent BL** far downstream of the critical streamwise transition point shown in Fig. 11).

2.4.1. Approximate Analytical Solution for a Turbulent ZPG BL based on the BL Integral Equation (pp. 439-440)

Similar to the previous approximate analytical solution for a laminar ZPG BL using the BL integral equation (cf. subsection 2.2.4), the BL integral equation can be also used for studying a turbulent BL. It should be indicated that when we derived the BL integral equation, no assumption has been made on whether the flow should be laminar or turbulent.

In full analogy to the previous ZPG laminar BL solution presented in subsection 2.2.4, we begin with the BL integral equation (Eq.(55) or Eq. (59)), i.e.

$$\tau_w = \rho U^2 \frac{d\theta}{dx} = \rho U^2 \frac{d\delta}{dx} \int_0^1 \frac{u}{U}\left(1 - \frac{u}{U}\right) d\eta \quad . \tag{59}$$

Furthermore, similar to the assumption made for the laminar ZPG BL velocity profile (cf. Eq. (62)), we also need to make an assumption for the turbulent ZPG BL velocity profile. In literature, it is popular to assume that a turbulent ZPG BL velocity profile follows the **one-seventh-power law**, viz.

$$\boxed{\frac{u}{U} = \left(\frac{y}{\delta}\right)^{1/7}} \quad . \tag{85}$$

In comparison with the laminar ZPG BL solution presented in subsection 2.2.4, a major difference between a laminar and a turbulent BL is in their assumed velocity profiles, represented by Eq. (62) and Eq. (85), respectively. It is understood that both these velocity profile equations are just assumptions, and therefore, solutions from the BL integral equation based on these assumed velocity profiles may deviate from the exact solutions (recall that the exact laminar BL solution is Blasius' solution). A significant flaw in the assumed turbulence BL velocity profile (represented by Eq. (85)) is that this one-seventh-power law holds in the entire turbulent BL except for the immediate vicinity of the wall, because it predicts that

$$\tau_w = \mu \frac{\partial u}{\partial y}\bigg|_{y=0} = \mu \left.\frac{U}{7\,\delta^{1/7}\,y^{6/7}}\right|_{y=0} \to \infty \quad , \tag{86}$$

which is not realistic. In order to fix the problem, we use the fully-developed velocity profile of a turbulent pipe flow to calculate τ_w for this case of a turbulent BL over a flat plate. This is, of course, another assumption. It is based on the fact that wall friction shear stress in a fully-developed pipe flow is similar to that in a fully-developed turbulent BL over a flat plate. As such, we have the following wall friction shear stress

$$\tau_w = 0.0233 \rho U^2 \left(\frac{\nu}{U\delta}\right)^{1/4} \quad , \tag{87}$$

which directly leads to the following result on the local skin friction coefficient

$$C_f = \frac{\tau_w}{\frac{1}{2}\rho U^2} = 0.0466 \left(\frac{\nu}{U\delta}\right)^{1/4} \quad . \tag{88}$$

By substituting the assumed profiles for $\frac{u}{U}$ (cf. Eq. (85)) and τ_w (cf. Eq. (87)) into the integral equation (59), we obtain

$$0.0233 \rho U^2 \left(\frac{\nu}{U\delta}\right)^{1/4} = \frac{d\delta}{dx} \int_0^1 \eta^{1/7}(1 - \eta^{1/7}) d\eta = \frac{7}{72}\frac{d\delta}{dx} \quad . \tag{89}$$

Integrating gives

$$\frac{4}{5}\delta^{5/4} = 0.240 \left(\frac{\nu}{U}\right)^{1/4} x + C \quad . \tag{90}$$

If we further assume that $\delta = 0$ at $x = 0$ (this is equivalent to assuming that the turbulent BL flow starts from the leading edge of the plate), then $C = 0$ and

$$\delta = 0.382 \left(\frac{\nu}{U}\right)^{1/5} x^{4/5} \quad . \tag{91}$$

Note that the above equation shows that the turbulent BL thickness grows as $x^{4/5}$. In comparison, from the previous discussions (see Eq. (75)), we know that the laminar BL thickness grows as $\sqrt{x}$. Similar to the laminar result (Eq. (75)), the above result on turbulent BL thickness can be rearranged to

$$\frac{\delta}{x} = 0.382 \left(\frac{\nu}{Ux}\right)^{1/5} = \boxed{\frac{0.382}{Re_x^{1/5}}} \quad . \tag{92}$$

Substituting the above result on δ into Eq. (88), we obtain

$$\boxed{C_f = \frac{0.0594}{Re_x^{1/5}}} \quad . \tag{93}$$

Similar to the previous results for a laminar BL (Eqs. (79-84)), for a turbulent BL, once the velocity profile is specified (i.e., once the one-seventh-power law (cf. Eq. (85)) is assumed), parameters such as displacement thickness δ^*, momentum thickness θ and shape factor H can be readily calculated.

Displacement thickness δ^*:

$$\begin{aligned} \delta^* = \int_0^\delta \left(1 - \frac{u}{U}\right) dy &= \delta \int_0^1 \left(1 - \frac{u}{U}\right) d\eta \\ &= \delta \int_0^1 (1 - \eta^{1/7}) d\eta \\ &= \frac{1}{8}\delta \quad , \end{aligned} \tag{94}$$

or, $\boxed{\frac{\delta^*}{\delta} = \frac{1}{8}}$. Based on Eq. (92), displacement thickness δ^* can be expressed

$$\frac{\delta^*}{x} = \frac{1}{8}\frac{0.382}{Re_x^{1/5}} = \frac{0.0478}{Re_x^{1/5}} \quad . \tag{95}$$

Momentum thickness θ:

$$\begin{aligned} \theta = \int_0^\delta \frac{u}{U}\left(1 - \frac{u}{U}\right) &= \delta \int_0^1 \frac{u}{U}\left(1 - \frac{u}{U}\right) d\eta \\ &= \delta \int_0^1 \eta^{1/7}\left[1 - \eta^{1/7}\right] d\eta \\ &= \frac{7}{72}\delta \quad , \end{aligned} \tag{96}$$

or, $\boxed{\frac{\theta}{\delta} = \frac{7}{72}}$. From Eq. (92), we further obtain

$$\frac{\theta}{x} = \frac{7}{72}\frac{0.382}{Re_x^{1/5}} = \frac{0.0371}{Re_x^{1/5}} \quad . \tag{97}$$

Shape factor H:

$$H = \frac{\delta^*}{\theta} = \left(\frac{1}{8}\delta\right) \Big/ \left(\frac{7}{72}\delta\right) = \frac{9}{7} = 1.286 \quad . \tag{98}$$

2.4.2. Turbulent BL Structure and the Law-of-the-Wall

As shown in Fig. 11, vertically, a turbulent BL can be divided into two distinct regions:
(I) inner layer, where the flow significantly influenced by the wall viscous effects; and
(II) outer layer, where the wall effects are almost non-existent and the flow behaves like a wake.
Within the inner layer, three layers can be further identified:
(i) viscous sublayer;
(ii) buffer layer;
(iii) overlap layer (also referred to as the "logarithmic layer").

The turbulent BL structure and physical properties of each layer are summarized as follows:

- **Inner layer:**
  - **viscous sublayer:** viscous shear stress τ_{vis} dominates, and turbulent shear stress τ_{turb} is negligible;
  - **buffer layer:** both viscous shear stress τ_{vis} and turbulent shear stress τ_{turb} are important, and they are of similar magnitudes;
  - **overlap layer:** both viscous shear stress τ_{vis} and turbulent shear stress τ_{turb} are important, but the magnitude of τ_{turb} is much larger than that of τ_{vis}.
- **Outer layer:** turbulent shear stress τ_{turb} dominates, and viscous shear stress τ_{vis} is negligible.

The velocity profile of a turbulent BL can be described using the so-called "**Law-of-the-wall**" based on the following **wall coordinates**:

$$\boxed{y^+ = \frac{u^* y}{\nu}} \quad , \tag{99}$$

where u^* is the so-called "**wall friction velocity**", defined as

$$\boxed{u^* = \sqrt{\frac{\tau_w}{\rho}}} \quad . \tag{100}$$

Using the u^*, the velocity of the BL flow can be non-dimensionalized as

$$\boxed{u^+ = \frac{\bar{u}}{u^*}} \quad . \tag{101}$$

With the wall coordinates defined above, the velocity profile of a ZPG turbulent BL in the inner layer can be generalized using the following functional relationship

$$\boxed{u^+ = f(y^+)} \quad . \tag{102}$$

► In a ZPG turbulent BL, the **viscous sublayer** exists for $0 < y^+ < 5$. Within the viscous sublayer, the non-dimensional velocity profile can be described using the following linear functional relationship

$$\boxed{u^+ = y^+} \quad (\text{for } 0 < y^+ < 5). \tag{103}$$

► Immediately outside of the viscous sublayer, the **buffer layer** exists within $5 < y^+ < 30$. The non-dimensional velocity profile u^+ within the buffer layer mostly relies on curve fitting, because an analytical formula is not readily available for describing the relationship between u^+ and y^+.

► Immediately outside of the buffer layer, the overlap layer exists for $y^+ > 30$ for a ZPG turbulent BL, and the non-dimensional velocity profile follows the so-called **logarithmic-law** for the overlap layer.

$$\boxed{u^+ = \frac{1}{\kappa} \ln y^+ + 5.0} \quad (\text{for } \; y^+ > 30). \tag{104}$$

where, $\boxed{\kappa = 0.41}$ is the "**von Kármán constant**".

► Outside of the overlap layer is the outer layer, where the turbulent shear stresses dominate, and the influence from the wall on the velocity is negligible in this region. In the outer layer, the flow behaves like a wake relative to the free stream and cannot be well represented using the wall coordinate (which relies on the wall friction velocity u^*). The discussion of the outer region shall be skipped as it is beyond the scope of this class.

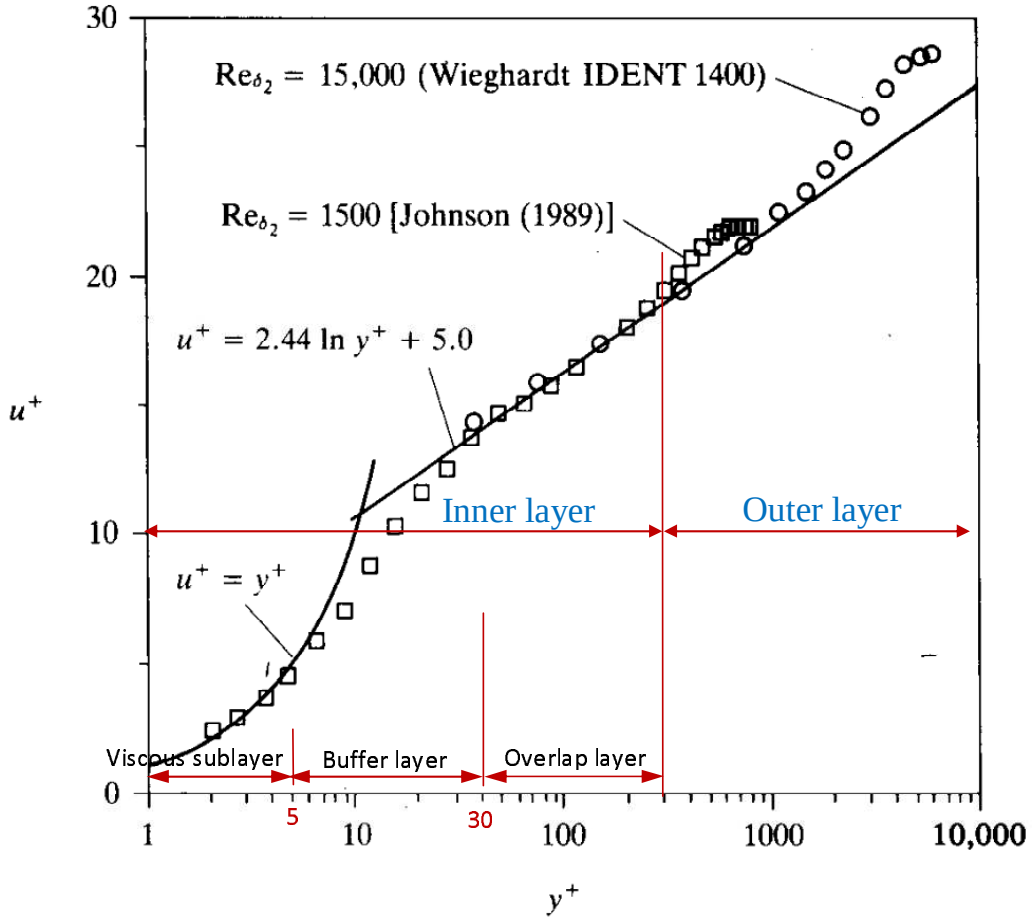

Fig. 12: The law-of-the-wall for a fully-developed ZPG turbulent boundary layer (source of figure [7]).

von Kármán's Two-Layer Turbulent BL Model

In order to further use Prandtl's mixing-length theory to the analysis of a steady fully-developed ZPG turbulent BL, von Kármán proposed a **two-layer turbulent BL model**, which assumes that a turbulent BL consists of only two layers: the viscous sublayer and the overlap layer (or, logarithmic layer). The buffer layer and outer layer are not included in consideration. In this two-layer turbulent BL model of von Kármán, the "transition" from the viscous sublayer to the overlap layer occurs at $y^+ = 10.8$. Figure 13 shows the simplified turbulent BL structure based on the two-layer model of von Kármán.

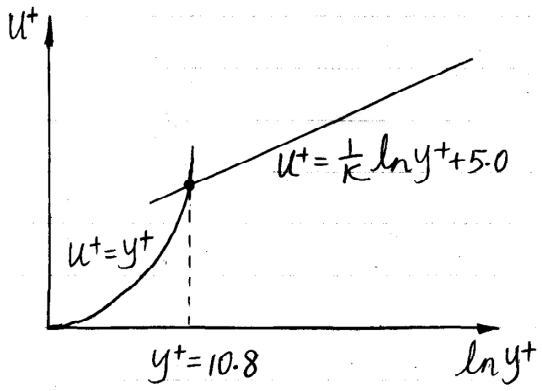

Fig. 13: von Kármán's **two-layer turbulent BL model** for a fully-developed ZPG turbulent boundary layer. It assumes that a ZPG turbulent BL consists of only two layers: the viscous sublayer and the overlap layer. The buffer layer and outer layer are not included in consideration. In this two-layer turbulent BL model of von Kármán, the "transition" from the viscous sublayer to the overlap layer occurs at $y^+ = 10.8$.

2.4.3. Turbulent BL Differential Equations

To investigate the a turbulent BL flow, it can be useful to check its x-momentum equation. The x-momentum equation for a laminar BL flow represented by Eq. (19) and Eq. (20) needs to be modified to

$$\boxed{\rho\left(\bar{u}\frac{\partial \bar{u}}{\partial x} + \bar{v}\frac{\partial \bar{u}}{\partial y}\right) = \rho U\frac{\partial U}{\partial x} + \frac{\partial \tau_{\text{tot}}}{\partial y}} \quad , \tag{105}$$

with

$$\boxed{\tau_{\text{tot}} = \tau_{\text{vis}} + \tau_{\text{turb}} = \mu\frac{\partial \bar{u}}{\partial y} - \rho\overline{u'v'}} \quad . \tag{106}$$

where $\bar{u}$ and $\bar{v}$ represent the Reynolds-averaged velocity fields.

Comments:

► The above x-momentum equation for a 2-D turbulent BL flow is similar to that for a 2-D laminar BL flow (i.e., Eq. (19)), expect that τ_{tot} now consists of two parts: viscous and turbulent shear stresses.

► The above x-momentum equation for a 2-D turbulent BL flow is fully-consistent with the 3-D turbulent flow case described by Eqs. (6) and (7). Just that in a 2-D turbulent BL flow case, only 1 of the 9 components of the viscous shear and Reynolds shear stress tensors is needed (i.e., $\mu\frac{\partial \bar{u}}{\partial y}$ and $-\rho\overline{u'v'}$, respectively).

From the previous discussion of Boussinesq's assumption (cf. Eq. (11)) for 3-D turbulence, the concept of eddy viscosity can be also used here for a 2-D turbulent BL flow, which leads to

$$\tau_{\text{turb}} = -\rho\overline{u'v'} = \mu_t\left(\cancelto{0}{\frac{\partial \bar{v}}{\partial x}} + \frac{\partial \bar{u}}{\partial y}\right) \approx \mu_t\frac{\partial \bar{u}}{\partial y} \quad , \tag{107}$$

where μ_t is the eddy viscosity for modelling the effects of turbulent motions. Owing to the BL assumption $\frac{\partial \bar{v}}{\partial x} \ll \frac{\partial \bar{u}}{\partial y}$, $\frac{\partial \bar{v}}{\partial x}$ can be ignored in Eq. (107). With the introduction of eddy viscosity for modelling turbulent shear stress based on Eq. (107), the total shear stress represented by Eq. (106) can be expressed

$$\boxed{\tau_{\text{tot}} = \tau_{\text{vis}} + \tau_{\text{turb}} = (\mu + \mu_t)\frac{\partial \bar{u}}{\partial y}} \quad . \tag{108}$$

Similar to Eq. (12) for 3-D turbulence, the x-momentum equation for a 2-D turbulent BL represented by Eq. (105) can now be further expressed as

$$\boxed{\rho\left(\bar{u}\frac{\partial\bar{u}}{\partial x}+\bar{v}\frac{\partial\bar{u}}{\partial y}\right)=\rho U\frac{\partial U}{\partial x}+\frac{\partial}{\partial y}\left[(\mu+\mu_t)\frac{\partial\bar{u}}{\partial y}\right]} \quad . \tag{109}$$

Differential Equations for A Steady Turbulent Boundary-Layer

$$\begin{cases} \text{Continuity Equation: } \dfrac{\partial\bar{u}}{\partial x}+\dfrac{\partial\bar{v}}{\partial y}=0 \quad , \\ \text{Momentum Equation: } \begin{cases} \rho\left(\bar{u}\dfrac{\partial\bar{u}}{\partial x}+\bar{v}\dfrac{\partial\bar{u}}{\partial y}\right)=\rho U\dfrac{\partial U}{\partial x}+\dfrac{\partial}{\partial y}\left[(\mu+\mu_t)\dfrac{\partial\bar{u}}{\partial y}\right] \quad , \\ \dfrac{\partial\bar{p}}{\partial y}=0 \quad . \end{cases} \end{cases} \tag{110}$$

2.5. Boundary Layer Separation (pp. 442-445)

2.5.1. Role of Pressure Gradient in a BL

In the previous subsections, we have thoroughly studied laminar and turbulent BL flows under zero pressure gradients. In this subsection, we further examine the role of a pressure gradient in the BL development. As discussed previously, based on Prandtl's BL theory, the vertical pressure gradient is always zero in a BL, i.e. $\frac{\partial p}{\partial y}\equiv 0$. Furthermore, because $\frac{dp}{dx}=-\rho U\frac{dU}{dx}$ holds within a BL, specifying $\frac{dp}{dx}$ is equivalent to specifying $\frac{dU}{dx}$. Depending on the value of the streamwise pressure gradient $\frac{dp}{dx}$, we have the following three types of streamwise pressure gradients:

- Favorable Pressure Gradient (FPG): $\frac{dp}{dx}<0$ and $\frac{dU}{dx}>0$;
- Zero Pressure Gradient (ZPG): $\frac{dp}{dx}=0$ and $\frac{dU}{dx}=0$;
- Adverse Pressure Gradient (APG): $\frac{dp}{dx}>0$ and $\frac{dU}{dx}<0$.

Figure 14 shows how the pressure gradient along a BL can be changed by using a channel with a variable cross-sectional area. The relationship between pressure p and the free-stream velocity U is

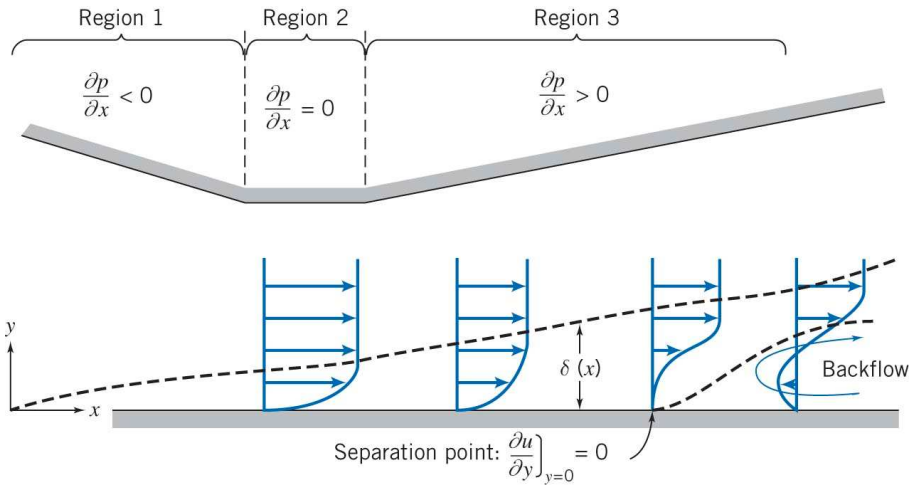

Fig. 14: Boundary-layer flow with three types of pressure gradients in a channel with a variable cross-sectional area.

governed by Bernoulli's equation.

► In region 1, the cross-sectional area decreases, and as such, the flow speeds up due to mass conservation. As a result, the pressure drops along the streamwise direction, forming a FPG BL.

► In region 2, the cross-sectional area remains constant, and therefore, both the flow velocity and pressure do not vary along the streamwise direction, resulting in a ZPG BL.

► In region 3, the cross-sectional area increases, causing the flow to decelerate and form a APG BL.

2.5.2. BL Separation Condition

As shown in Fig. 14, in region 3, if the magnitude of the APG is large enough, the BL may **separate** from the wall, accompanied with a reverse flow pattern (i.e., $u < 0$) in the vicinity of the wall, a negative wall friction shear stress (i.e., $\tau_w = \mu \frac{\partial u}{\partial y}|_{y=0} < 0$) and a negative local skin friction coefficient (i.e., $C_f = \tau_w/(\frac{1}{2}\rho U^2) < 0$).

► Right at the BL separation point (see Fig. 15(d)), the following **BL separation conditions** hold:

$$\boxed{\tau_w = 0\,, \quad C_f = 0\,, \quad \left.\frac{\partial u}{\partial y}\right|_{y=0} = 0} \quad . \tag{111}$$

► In a FPG BL, the pressure keeps dropping and the flow keeps accelerating in the streamwise direction. The flow cannot reverse its direction, BL never separates, and $\tau_w > 0$.

► In a ZPG BL, from Table 9.2 (see page 47), $C_f = \frac{0.664}{\sqrt{Re_x}} > 0$ (Blasius' exact solution), the flow never reverses in the near-wall region, and BL never separates.

► In an APG BL, the BL may separate, but not guaranteed. This is because the sign of τ_w depends also on other parameters than just the pressure gradient. In effect, from Eq. (52),

$$\frac{C_f}{2} = \frac{d\theta}{dx} + (2+H)\frac{\theta}{U}\frac{dU}{dx} \quad . \tag{52}$$

From this equation, it is understood that the sign of C_f (or the sign of τ_w) depends upon not only the pressure gradient (indicated by $\frac{dU}{dx}$), but also the shape factor H etc. Figure 15 gives a detailed description of the BL development under FPG, ZPG and APG. In Fig. 15(c)-(d), the BL is subjected to an APG, but the BL separates only when the APG is severe enough. This further confirms that APG is a necessary but not a sufficient condition for BL separation.

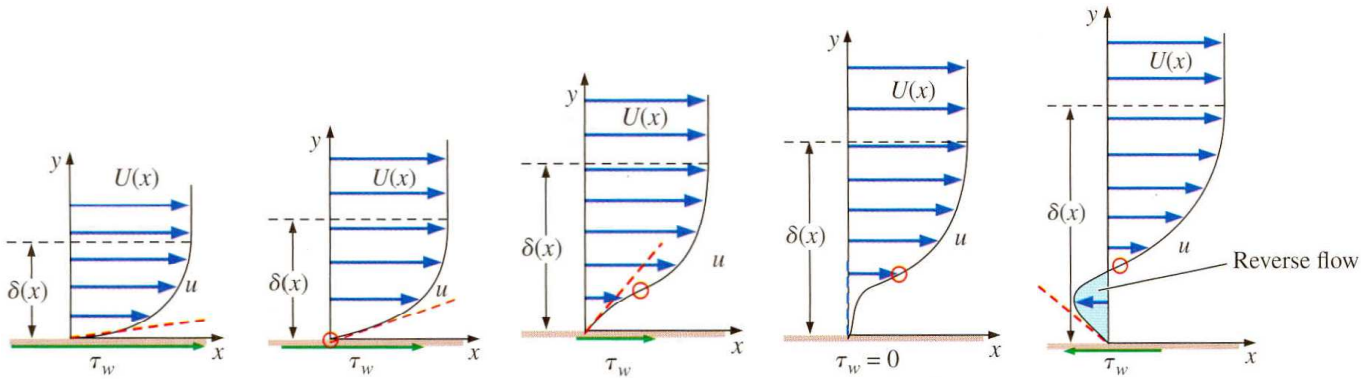

(a) FPG
$\frac{dp}{dx} < 0, \quad \frac{dU}{dx} > 0$
$\tau_w > 0$
No separation

(b) ZPG
$\frac{dp}{dx} = 0, \quad \frac{dU}{dx} = 0$
$\tau_w > 0$
No separation

(c) Mild APG
$\frac{dp}{dx} > 0, \quad \frac{dU}{dx} < 0$
$\tau_w > 0$
No separation

(d) Critical APG
$\frac{dp}{dx} > 0, \quad \frac{dU}{dx} < 0$
$\tau_w = 0$
Separation point

(e) Strong APG
$\frac{dp}{dx} > 0, \quad \frac{dU}{dx} < 0$
$\tau_w < 0$
Separated region

Fig. 15: BL velocity profiles under different pressure gradients $\frac{dp}{dx} = -\rho U \frac{dU}{dx}$ (source of figure [6]).

Good online teaching on BL development and separation:
https://www.youtube.com/watch?v=LvVuuaqCC7A
https://www.youtube.com/watch?v=e1TbkLIDWys
https://www.youtube.com/watch?v=6o-RbD1tlhs
https://www.youtube.com/watch?v=JcxOub0E4aA
https://www.youtube.com/watch?v=fCniTNB2ONQ

REFERENCES

[1] Pritchard, P. J. 2011, *Fox and McDonald's Introduction to Fluids Mechanics*, 8th edition, Wiley, USA.
[2] White, F. M. 2011, *Fluid Mechanics*, 7th edition, McGraw-Hill, New York, NY.
[3] Capra, F. 2007, *The Science of Leonardo*, Doubleday, New York, NY.
Web link: http://www.fritjofcapra.net/leonardo.html
[4] Reynolds, O. 1883, An experimental investigation of the circumstances which determine whether the motion of water in parallel channels shall be direct or sinuous and of the law of resistance in parallel channels, *Philos. Trans. R. Soc.*, vol. 174, pp. 935-982.
[5] Reynolds, O. 1895, On the dynamical theory of incompressible viscous fluids and the determination of the criterion. *Philos. Trans. R. Soc.*, vol. 186, pp. 123-164.
[6] Çengel, Y. A. and Cimbala J. M. 2014, *Fluid Mechanics: Fundamentals and Applications*, 3rd edition, McGraw-Hill, New York, NY.
[7] Kays, W., Crawford, M. and Weigand B. 2005, *Convective Heat and Mass Transfer*, 4th edition, McGraw-Hill, New York, NY.

Class Example

Purpose: understanding BL thickness, displacement thickness, momentum thickness, and integral equation

For a zero-pressure-gradient laminar BL flow over a flat plate, assume that the velocity profile is of a sinusoidal form: $u = a + b\sin(\frac{\pi}{2}\frac{y}{\delta}) + c\cos(\frac{\pi}{2}\frac{y}{\delta})$. Derive all the equations and parameters listed in row 5 of Table 9.2. Specifically, determine: (1) $\frac{u}{U}$; (2) τ_w; (3) non-dimensionalized BL thickness $\frac{\delta}{x}$ (as a function of Re_x); (4) C_f (as a function of Re_x); (5) $\frac{\delta^*}{\delta}$; (6) $\frac{\theta}{\delta}$; and (7) shape factor $H = \frac{\delta^*}{\theta}$.

Problem 2 [Follow the steps on PP. 14-18 of the notes]

(1) $u = a + b\sin\left(\frac{\pi}{2}\frac{y}{\delta}\right) + c\cos\left(\frac{\pi}{2}\frac{y}{\delta}\right)$

B.C. $\begin{cases} \text{at } y=0,\ u=0 \\ \text{at } y=\delta,\ u=U \\ \text{at } y=\delta,\ \frac{\partial u}{\partial y}=0 \end{cases} \Rightarrow \begin{cases} 0 = a + c \\ U = a + b \\ 0 = -\frac{c}{\delta} \end{cases} \Rightarrow \begin{cases} a = 0 \\ b = U \\ c = 0 \end{cases}$

$\therefore u = U\sin\left(\frac{\pi}{2}\frac{y}{\delta}\right)$

with non-dimensional coordinate $\frac{y}{\delta}$ & velocity $\frac{u}{U}$, we have

$$\frac{u}{U} = \sin\left(\frac{\pi}{2}\eta\right) \qquad \text{——— (1)}$$

(2) $\tau_w = \mu \left.\frac{\partial u}{\partial y}\right|_{y=0} = \frac{\mu U}{\delta} \left.\frac{d(u/U)}{d\eta}\right|_{\eta=0}$ [Eq.(64) from the notes]

$\therefore \tau_w = \frac{\mu U}{\delta}\left[\frac{d}{d\eta}\left(\sin\left(\frac{\pi}{2}\eta\right)\right)\right]_{\eta=0} = \frac{\mu U}{\delta}\cdot\left[\frac{\pi}{2}\cos\left(\frac{\pi}{2}\eta\right)\right]_{\eta=0} = \frac{\pi}{2}\frac{\mu U}{\delta}$ ——— (2)

(3) From the momentum Integral Eqn for a ZPG BL [i.e. Eq.(57) in the notes],

$$\tau_w = \rho U^2 \frac{d\theta}{dx} = \rho U^2 \frac{d\delta}{dx}\int_0^1 \frac{u}{U}\left(1 - \frac{u}{U}\right) d\eta$$

substituting Eqs.(1) & (2) into the above eqn,

$$\frac{\pi}{2}\frac{\mu U}{\delta} = \rho U^2 \frac{d\delta}{dx}\int_0^1 \sin\left(\tfrac{\pi}{2}\eta\right)\cdot\left[1 - \sin\left(\tfrac{\pi}{2}\eta\right)\right] d\eta$$

$$= \rho U^2 \frac{d\delta}{dx}\int_0^1 \left[\sin\left(\tfrac{\pi}{2}\eta\right) - \sin^2\left(\tfrac{\pi}{2}\eta\right)\right] d\eta$$

$$= \rho U^2 \frac{d\delta}{dx}\int_0^1 \left[\sin\left(\tfrac{\pi}{2}\eta\right) - \tfrac{1}{2} + \tfrac{1}{2}\cos(\pi\eta)\right] d\eta$$

$$= \rho U^2 \frac{d\delta}{dx}\left[-\tfrac{2}{\pi}\cos\left(\tfrac{\pi}{2}\eta\right) - \tfrac{1}{2}\eta + \tfrac{1}{2\pi}\sin(\pi\eta)\right]_0^1$$

$$= \rho U^2 \frac{d\delta}{dx}\left(\frac{2}{\pi} - \frac{1}{2}\right)$$

Note that: $\sin^2\alpha = \frac{1}{2}(1 - \cos 2\alpha)$

Or, $\delta\, d\delta = \frac{\pi^2}{4-\pi}\frac{\mu}{\rho U}\, dx$

Integrating, $\frac{1}{2}\delta^2 = \frac{\pi^2}{4-\pi}\frac{\mu}{\rho U}x + C$

Assume that $\delta = 0$ at $x = 0$, we have $c = 0$.

Therefore, $\frac{1}{2}\delta^2 = \frac{\pi^2}{4-\pi}\frac{\mu}{\rho U}x$

Introducing $Rex = \frac{\rho U x}{\mu}$, the above equation becomes

$$\frac{1}{2}\delta^2 = \frac{\pi^2}{4-\pi}\frac{\mu}{\rho U x}x^2$$

or, $$\frac{\delta^2}{x^2} = \frac{2\pi^2}{4-\pi}\frac{1}{Rex}$$

or, $$\frac{\delta}{x} = \sqrt{\frac{2\pi^2}{4-\pi}}\cdot\frac{1}{\sqrt{Rex}} = \frac{4.80}{\sqrt{Rex}} \quad \text{——— (3)}$$

(4) $$C_f = \frac{\tau_w}{\frac{1}{2}\rho U^2} = \frac{\frac{\pi}{2}\frac{\mu U}{\delta}}{\frac{1}{2}\rho U^2} = \frac{\pi\mu}{\rho U\delta} = \frac{\pi\mu}{\rho U x}\frac{x}{\delta} = \frac{\pi}{Rex}\frac{x}{\delta}$$

Substituting Eq(3) into the above equation, we obtain,

$$C_f = \frac{\pi}{Rex}\cdot\frac{\sqrt{Rex}}{4.80} = \frac{0.654}{\sqrt{Rex}} \quad \text{——— (4)}$$

(5) Displacement thickness

$$\delta^* = \int_0^\delta (1-\frac{u}{U})dy = \delta\int_0^1 (1-\frac{u}{U})d\eta$$

$$= \delta\int_0^1 [1-\sin(\tfrac{\pi}{2}\eta)]\,d\eta$$

$$= \delta\cdot[1-\tfrac{2}{\pi}]$$

$$= \tfrac{\pi-2}{\pi}\delta$$

$$\therefore \frac{\delta^*}{\delta} = \frac{\pi-2}{\pi} \quad \text{——— (5)}$$

(6) Momentum thickness

$$\theta = \int_0^\delta \frac{u}{U}(1-\frac{u}{U})dy = \delta\cdot\int_0^1 \frac{u}{U}(1-\frac{u}{U})d\eta$$

$$= \delta\cdot\int_0^1 \sin(\tfrac{\pi}{2}\eta)\cdot[1-\sin(\tfrac{\pi}{2}\eta)]\,d\eta$$

$$= \delta\cdot(\tfrac{2}{\pi}-\tfrac{1}{2})$$

$$= \delta\cdot\tfrac{4-\pi}{2\pi}$$

↑ Note that this integral has already been worked out in step (3)

$$\therefore \frac{\theta}{\delta} = \frac{4-\pi}{2\pi} \quad \text{——— (6)}$$

(7) Shape factor

$$H = \frac{\delta^*}{\theta} = \left(\frac{\pi-2}{\pi}\delta\right) \Big/ \left(\frac{4-\pi}{2\pi}\delta\right) = \frac{2\pi-4}{4-\pi} = 2.66$$

Problem 9.23

[Difficulty: 2]

9.23 Laboratory wind tunnels have test sections 25 cm square and 50 cm long. With nominal air speed $U_1 = 25$ m/s at the test section inlet, turbulent boundary layers form on the top, bottom, and side walls of the tunnel. The boundary-layer thickness is $\delta_1 = 20$ mm at the inlet and $\delta_2 = 30$ mm at the outlet from the test section. The boundary-layer velocity profiles are of power-law form, with $u/U = (y/\delta)^{1/7}$. Evaluate the freestream velocity, U_2, at the exit from the wind-tunnel test section. Determine the change in static pressure along the test section.

Given: Data on wind tunnel and boundary layers

Find: Uniform velocity at exit; Change in static pressure through the test section

Solution:

Basic equations $\dfrac{\partial}{\partial t}\int_{CV}\rho\, d\mathcal{V} + \int_{CS}\rho\vec{V}\cdot d\vec{A} = 0$ (4.12) $\delta_{disp} = \displaystyle\int_0^{\delta}\left(1 - \frac{u}{U}\right)dy$ $\dfrac{p}{\rho} + \dfrac{V^2}{2} + g\cdot z = \text{const}$

Assumptions: 1) Steady flow 2) Incompressible 3) No friction outside boundary layer 4) Flow along streamline 5) Horizontal

For this flow $\rho\cdot U\cdot A = \text{const}$ and $\dfrac{u}{U} = \left(\dfrac{y}{\delta}\right)^{\frac{1}{7}}$

The given data is $U_1 = 25\cdot\dfrac{m}{s}$ $h = 25\cdot cm$ $A = h^2$ $A = 625\cdot cm^2$

We also have $\delta_1 = 20\cdot mm$ $\delta_2 = 30\cdot mm$

Hence $\delta_{disp} = \displaystyle\int_0^{\delta}\left(1 - \frac{u}{U}\right)dy = \int_0^{\delta}\left[1 - \left(\frac{y}{\delta}\right)^{\frac{1}{7}}\right]dy = \delta\cdot\int_0^{1}\left(1 - \eta^{\frac{1}{7}}\right)d\eta$ where $\eta = \dfrac{y}{\delta}$ $\delta_{disp} = \dfrac{\delta}{8}$

Hence at the inlet and exit

$\delta_{disp1} = \dfrac{\delta_1}{8}$ $\delta_{disp1} = 2.5\cdot mm$ $\delta_{disp2} = \dfrac{\delta_2}{8}$ $\delta_{disp2} = 3.75\cdot mm$

Hence the areas are $A_1 = \left(h - 2\cdot\delta_{disp1}\right)^2$ $A_1 = 600\cdot cm^2$

$A_2 = \left(h - 2\cdot\delta_{disp2}\right)^2$ $A_2 = 588\cdot cm^2$

Applying mass conservation between Points 1 and 2

$\left(-\rho\cdot U_1\cdot A_1\right) + \left(\rho\cdot U_2\cdot A_2\right) = 0$ or $U_2 = U_1\cdot\dfrac{A_1}{A_2}$ $U_2 = 25.52\,\dfrac{m}{s}$

The pressure change is found from Bernoulli $\dfrac{p_1}{\rho} + \dfrac{U_1^2}{2} = \dfrac{p_2}{\rho} + \dfrac{U_2^2}{2}$ with $\rho = 1.21\cdot\dfrac{kg}{m^3}$

Hence $\Delta p = \dfrac{\rho}{2}\cdot\left(U_1^2 - U_2^2\right)$ $\Delta p = -15.8\,Pa$ The pressure drops slightly through the test section